COUPLING PHOTODRIVEN MULTIELECTRON REDUCTION OF RUTHENIUM POLYPYRIDYL COMPLEXES WITH HYDROGEN EVOLVING CO-CATALYSTS

by

CALE MCALISTER

Presented to the Faculty of the Graduate School of

The University of Texas at Arlington in Partial Fulfillment

of the Requirements for the Degree of

MASTER OF SCIENCE IN CHEMISTRY

THE UNIVERSITY OF TEXAS AT ARLINGTON

May 2007

ACKNOWLEDGEMENTS

I would like to thank my research advisor, Dr. MacDonnell for the opportunity to be involved in this research, and also for advice, encouragement, and guidance throughout the course of my research. I would also like to thank Dr. Norma Tacconi for all of her advice, and her eagerness to help out in any way she could.

I would like to thank all of my fellow lab members for all of their help and encouragement in my research, for their input and ideas, and for their willingness to lend a helping hand. A special thanks goes out to T.J. Lane and Matthias Schwalbe for their assistance and contributions to my research.

Above all, I would like to thank my wife, Renae, for her love and support as I've endeavored to continue my education.

April 17, 2007

ABSTRACT

COUPLING PHOTODRIVEN MULTIELECTRON REDUCTION
OF RUTHENIUM POLYPYRIDYL COMPLEXES WITH
HYDROGEN EVOLVING CO-CATALYSTS

Publication No. _____

Cale McAlister, M.S.

The University of Texas at Arlington, 2007

Supervising Professor: Frederick M. MacDonnell

With energy demands continuing to increase, the importance of finding a means of converting solar energy into a usable form of chemical energy continues to escalate. Photocatalysis provides a viable approach to harnessing energy from the sun for its use in energy converting reactions such as the water splitting reaction. Ruthenium polypyridyl complexes have played an important role in the growth and advancement of artificial photosynthetic systems, many of which have the ability to utilize solar energy in the process of H_2 evolution.

This thesis focuses on a biomimetic approach to solar H_2 production through multi-electron photocatalysis. The two dinuclear Ruthenium complexes $[(phen)_2Ru(tatpp)Ru(phen)_2]^{4+}$ and $[(phen)_2Ru(tatpq)Ru(phen)_2]^{4+}$ both have the ability to undergo multiple reductions and store those electrons on the central bridging ligand of each respective complex. These complexes have been investigated as possible photocatalyst and have been found to evolve H_2 under the given conditions for extended periods of time. The photocatalytic lifetime of these complexes has been shown to be significantly longer than many of the standard Ruthenium polypridyl photocatalyst.

TABLE OF CONTENTS

Appendix

LIST OF ILLUSTRATIONS

LIST OF TABLES

LIST OF SCHEMES

CHAPTER 1

INTRODUCTION

1.1 Background

It has become abundantly clear that the world is in need of alternative energy sources that will ease the overwhelming dependence on fossil fuels that has been accrued in the last century. The environmental issues, increase in price, decrease in reliability, political strains, and eventual stockpile depletion all support the fact that fossil fuels will not be a viable choice to support the world economy in the future. Finding an ample source of clean energy is a pressing need in the world about us.[1]

The largest and most readily available energy source that we have access to today is one that we barely utilize at all. Within one hour, the Earth is struck with 4.3×10^{20} J of energy from the sun, while the total amount of energy consumed in one year by the entire world equals 4.1×10^{20} J.[1] The ability to harness even a small portion of this energy would greatly decrease the dependency on fossil fuels.

Assuming we develop methods to harness this energy, another important issue is how is the harnessed energy to be stored. Many scientists believe the best approach would be to use solar energy to split water into O_2 and H_2 (see Eq. 1.1).[2] Hydrogen is

$$2\ H_2O \rightarrow O_2 + 2\ H_2 \qquad \Delta G = 474\ \text{kJ/mol} = 4.92\ \text{eV} \qquad \text{Eq 1.1}$$

an extremely promising fuel and O_2 is an environmentally friendly and commercially useful by-product. Hydrogen has a number of advantages over other possible fuels. For example, it is carbon-free and therefore its combustion does not add CO_2 to the

atmosphere. It has a fuel value that is approximately triple (142MJ kg^{-1}) that found in liquid hydrocarbons (47 MJ kg^{-1}) and is an ideal fuel for fuel cells.[3]

The development and use of H_2 as a viable fuel has been discussed in many different forums.[1,2,4-7] While the question remains as to how to produce H_2 in an efficient and inexpensive manner, it is clear that utilizing the naturally abundant resources of water and solar energy is an ideal solution to many of our energy problems.

The development of photocatalytic systems capable of driving the water splitting reaction (WSR) remains a challenging task, however natural photosynthesis shows us that such processes are not only possible but can be done under relatively mild conditions. Photosynthesis is the natural process in which plants and some bacteria absorb solar energy and use it to produce molecules with strong reducing potentials (Eq 1.3), high energy molecules (Eq 1.4), and ultimately to produce fuel in the form of carbohydrates (Eq 1.5).[8,9] The electrons necessary to carry out Eq 1.3 and Eq 1.5 come from the oxidation of water molecules, with O_2 released into the atmosphere as the by-product. The photosynthetic apparatus in plants is composed of a membrane-bound, highly ordered molecular assemblies of proteins and co-factors that function to efficiently harvest solar energy, funnel this energy to a centrally-located pair of chlorophyll molecules which undergoes electron transfer reactions with associated donor and acceptor molecules such that the electron and resulting hole are efficiently separated. It is the energy inherent in this charge-separated (cs) state that is used to transform small molecule substrates into the desired product.[10-12]

$$NADP^+ + 2e^- + H^+ \rightarrow NADPH \qquad \text{Eq 1.3}$$

$$ADP + P_i \rightarrow ATP + H_2O \qquad \text{Eq 1.4}$$

$$6\,CO_2 + 6\,H_2O \rightarrow C_6H_{12}O_6 + 6\,O_2 \qquad \text{Eq 1.5}$$

Molecular and supramolecular systems designed to mimic the natural photosynthetic system in function are often referred to as "artificial photosynthetic systems". To date, no molecular system has proved directly capable of driving the WSR however, a number of artificial photosystems are capable of mimicking many of the individual steps found in photosynthesis, such as antenna-like energy capture and transfer, photocatalytic hydrogen generation, etc.[7,11-22] A supramolecular photosystem capable of splitting water will need at least three major components: 1) a chromaphore able to harvest solar energy, 2) a catalyst for the OER and 3) a catalyst for the HER (Figure 1.1). Furthermore these three components must be able to efficiently transfer electrons between components to drive the overall reaction.

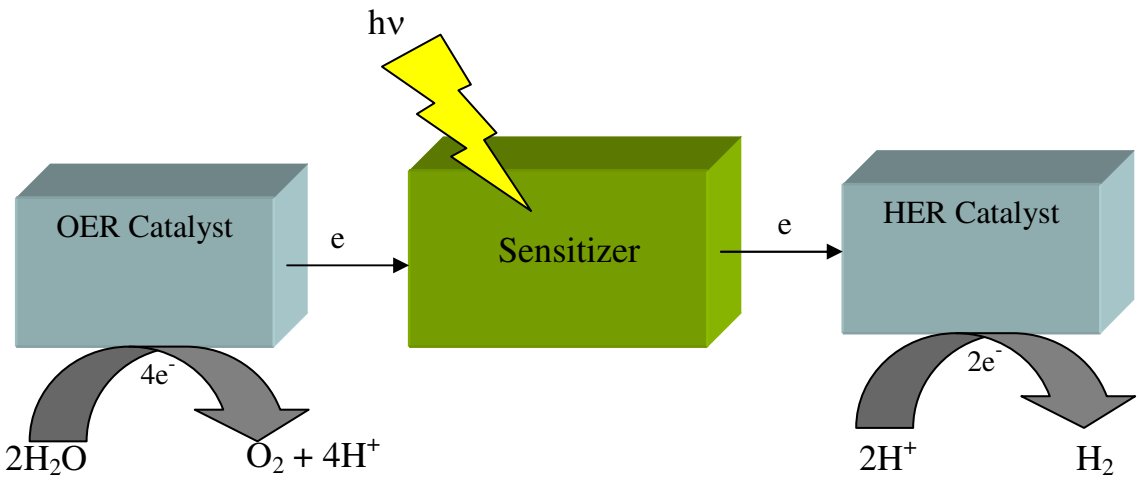

Figure 1.1 Basic example of a supramolecular photosystem.

1.2 Water Splitting Energetics

As seen in Eq 1.1, the energetic threshold that must be met in order to evolve one molecule of O_2 is 4.92 eV. Since this reaction requires this amount of energy, naturally one would attempt to use a higher energy source of light to drive this reaction. Photocatalytic systems utilizing UV light have been designed and investigated for many years,[23-25] but these systems are not practical because only 4% of the solar radiation that strikes the earth's surface is in the UV. On the other hand, solar radiation in the visible range (400 – 750 nm) is far more abundant. These photons have energies ranging from 1.65 eV to 3.1 eV[26] and thus at least two photons are required to drive the WSR. In addition to the energy needed to split water, the reaction requires the transfer of multiple electrons from the site of oxidation to the site of reduction as can be seen clearly upon inspecting its half reactions, which are referred to as the hydrogen evolving reaction (Eq 1.6) and the oxygen evolving reaction (Eq 1.7).[27,28]

$$2\ H^+ + 2\ e^- \rightarrow\ H_2 \qquad \Delta G = 79.9\ kJ/mol\ H_2 \qquad \text{Eq 1.6}$$

$$2\ H_2O \rightarrow\ O_2 + 4\ H^+ + 4\ e^- \qquad \Delta G = 314.9\ kJ/mol\ O_2 \qquad \text{Eq 1.7}$$

The multi-electron nature of Eq 1.6 and 1.7 further complicates the efforts to mimic photosynthesis on the molecular level. Since water cannot absorb visible radiation, these artificial photosystems must incorporate a chromaphore with the ability to harvest visible solar energy. Most generally, a chromaphore that has absorbed a photon is followed by the excitation of a single electron. No matter the amount of energy associated with this electron, it cannot drive either of these half reactions due to their multi-electron requirements. This issue is resolved in nature by a tetramanganese

cofactor found within photosystem II that stores electrons until the multi-electron requirement for O_2 evolution is met.[29] In the same sense, a molecular photosystem needs a collection site in which oxidation or reduction equivalents can be stored and utilized in multi-electron reactions. Due to the complexity of the photosystem that is required to carry out the water splitting reaction, the majority of the efforts made in this area of research have been focused on one of the two half reactions.[27]

1.3 Ruthenium Polypyridyl Complexes

Photosystems need to include a chromaphore that is resistant to photodecomposition and upon photoexcitation forms a long-lived charge-separated state. The other components of the supramolecular system must be able to react with this photoexcited chromophore to extract the energy of the excited state and restore the chromophore to its original state. While many transition metal complexes,[30-33] metalloporphyrins,[34-36] and various other molecules have been investigated as chromaphores, most lack the functionality and robustness to be useful for the water splitting reaction.

Ruthenium (II) polypyridyl complexes have been extensively investigated in this area of research due to their increased stability and favorable photophysical properties.[10,14-20,37-41] The increased stability of these complexes is due to the significant covalent character of the Ru-N bonds as a result of their electronegativities (χ 2.2 for Ru, χ 3.0 for N), the π bond formed between polypyridyl ligand π-accepting orbitals and Ru t_{2g} orbitals, and also due to the electronic stabilization that accompanies low spin d^6 second row transition metals. These complexes also typically exhibit long excited state

lifetimes and strong absorption of visible light.[42-46] Many ruthenium (II) polypyridyl complexes have been synthesized and studied, which has shown the ability to tune the spectral properties of these complexes by simple ligand substitution. This is a valuable property of these complexes in that it allows the system to be adjusted for maximal light absorption.

The prototypical ruthenium (II) polypyridyl complex is $Ru(bpy)_3^{2+}$. It has been extensively studied and serves as a good example of the photophysical properties found in this family of complexes. This complex has a strong absorption band at 452 nm (ε = 13000 M^{-1} cm^{-1} in MeCN)[12] which corresponds to the Ru $d\pi \rightarrow$ bpy π^* MLCT transition. The luminescence of this molecule is due to the thermally equilibrated ^{3}MLCT excited state, which has a lifetime of ~1 μs.[47] The photoexcited complex, $Ru(bpy)_3^{2+*}$, can function as a strong oxidant or strong reductant.[45] Figure 1.2 shows the photoproducts formed upon electron transfer to or from $Ru(bpy)_3^{2+*}$.[12]

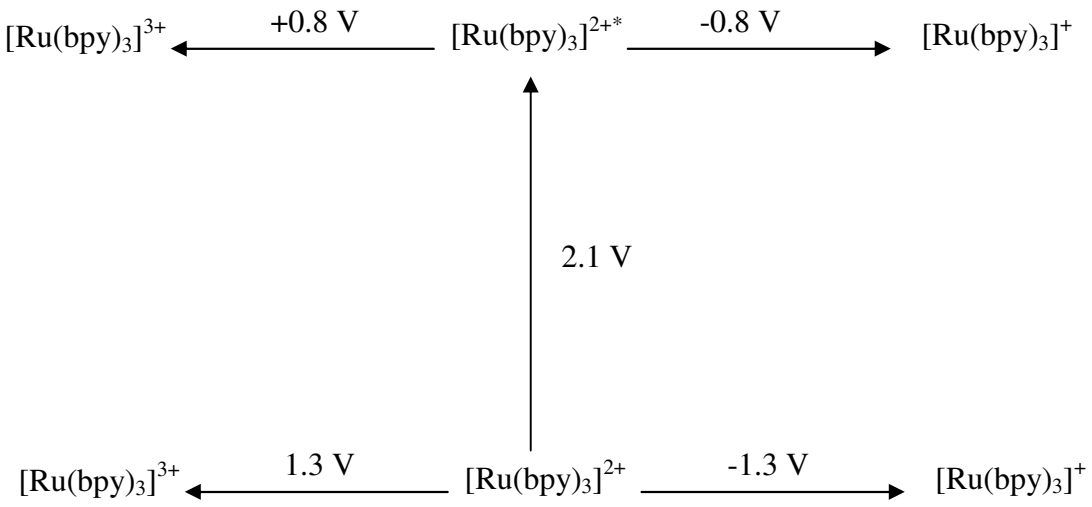

Figure 1.2 Latimer Diagram of excited and ground state redox potentials for $[Ru(bpy)_3]^{2+}$.

One of the limitations of $Ru(bpy)_3^{2+}$ as a photocatalyst is that it is only capable of driving single-electron reactions.[13] Since the water splitting reaction is a multi-electron process, such photocatalysts do not meet the stoichiometric requirements for these reactions. For this reason, many photosystems designed for H_2 evolution require an electron relay that is capable of storing electrons and subsequently transferring them to a H_2 evolving co-catalyst. In order for this system to be functional, the reduction potential of the electron relay needs to be lower than that of the sensitizer but higher than –0.414V, the reduction potential of H^+/H_2 couple at pH 7. Methyl viologen is a commonly used electron relay for such photochemical systems (Figure 1.3). With the reduction potential of $Ru(bpy)_3^{2+}$ being –0.84 V and that of MV^{2+}/MV^+ being –0.46 V, H_2 evolution is still thermodynamically possible with this electron relay.

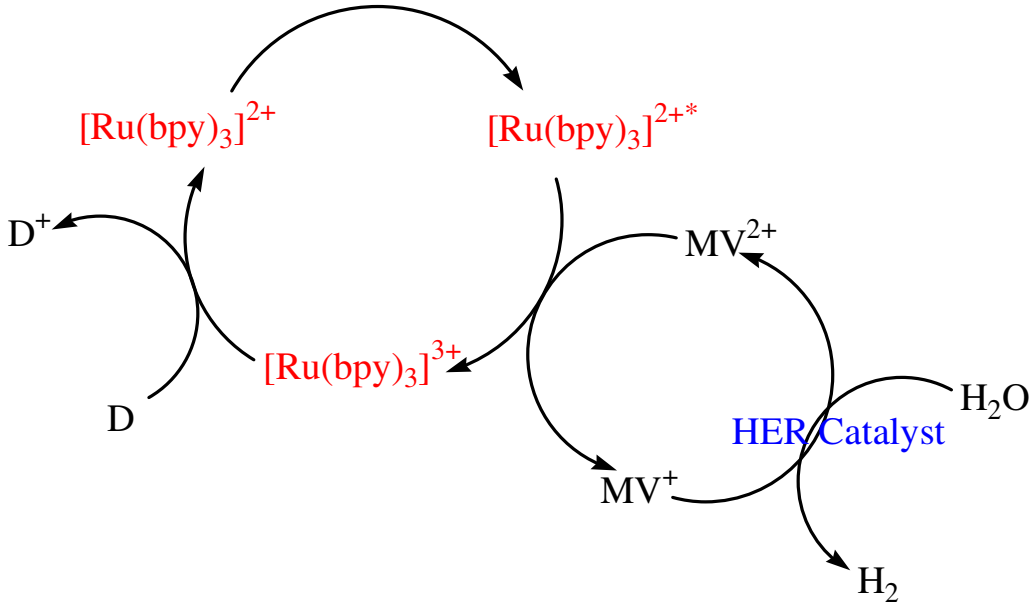

Figure 1.3 $[Ru(bpy)_3]^{2+}$ photosystem with MV^{2+} electron relay, catalyst for H_2 evolution, and sacrificial reducing agent D.

The species formed by addition or removal of an e^- from $[Ru(bpy)_3]^{2+*}$ can function catalytically in a reductive or oxidative quenching pathway to drive chemical reactions. This can be seen in Figure 1.4, where A and D represent acceptor and donor molecules, respectively.

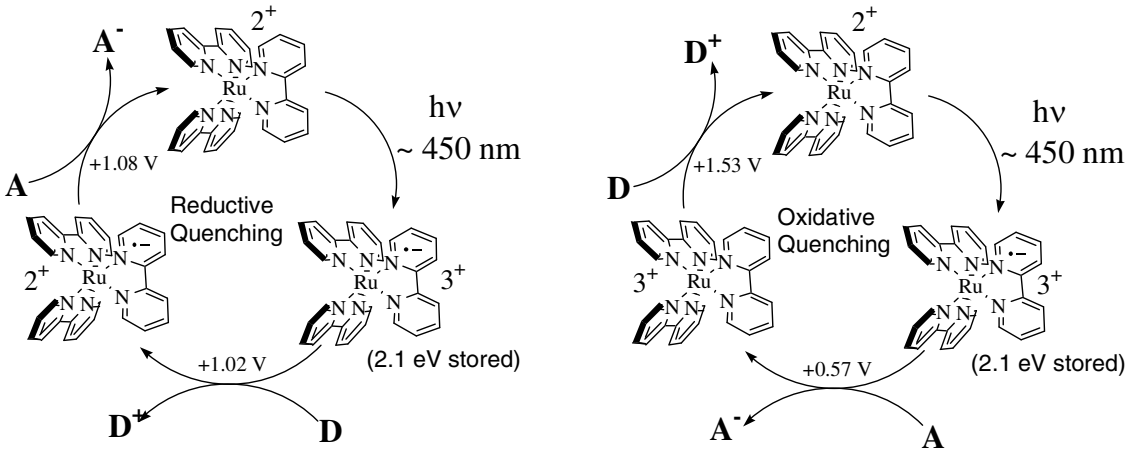

Figure 1.4 Catalytic reactions using $[Ru(bpy)_3]^{2+}$.

When $Ru(bpy)_3^{2+*}$ is quenched by electron transfer, its overall efficiency within this system is decreased due to the competing back-electron transfer process in which the ground state of the complex is reformed. This competing process wastes the excitation energy of $Ru(bpy)_3^{2+*}$ by regenerating the ground state instead of using it for subsequent chemical reactions. Efforts have been made to avoid this unproductive back reaction by providing a secondary pathway in which the photoexcited state of this complex can rapidly transfer its stored energy to another molecule to compete with the back reaction.[48-50]

In order to inhibit the non-productive back reaction within this system, a sacrificial reducing agent is used to reduce $Ru(bpy)_3^{3+}$ to $Ru(bpy)_3^{2+}$, and thus freeing the excited electron to be used in further chemical reactions. A number of electron donors and electron acceptors, such as TEA, TEOA, and $[Co(NH_3)_5Cl]^{2+}$ have been shown to readily decompose once the electron transfer has taken place, thus preventing any further non-productive back reactions.[51-53] While the electron relay serves it purpose in this system, it also introduces a number of new variables such as relay stability, selectivity towards co-catalysts, energy transfer loss, and formation of by-products that further complicate the system and decrease efficiency.[54] These photosystems are effective under the right conditions, but they still have their limitations.

1.4 Multi-electron Photocatalysts

The multi-electron nature of the water splitting reaction has posed a challenge in designing artificial photosystems due to the fact that photoexcitation is generally a one-electron process.[55] If the water splitting reaction was carried out one electron at a time, it would result in forming highly reactive intermediates (Eq 1.8 -1.9). The energy required to carry out these reactions are considerably higher when compared to the multi-electron reactions that require –0.414 V and –0.816 V for the H_2 and O_2 evolving reactions, respectively.[55,56]

$$H^+ + e^- \rightarrow H^\bullet \qquad \Delta G = -2.69 \text{ V} \qquad \text{Eq 1.8}$$

$$OH^- \rightarrow OH^\bullet + e^- \qquad \Delta G = -2.33 \text{ V} \qquad \text{Eq 1.9}$$

There are relatively few photoactive complexes that can undergo multiple photoreductions and thereby store more than one reducing electron at a time. One of the

first photoactive complexes able to store multiple electrons was a Ru^{II}-Ir^{III}-Ru^{II} trimer reported by Brewer et al (Figure 1.5).[57] Upon photoirradiation in the presence of a sacrificial reducing agent, this complex is able to store 2 electrons on the two bridging polypyridyl ligands. More recently, the same group has reported a Ru^{II}-Rh^{III}-Ru^{II} trimer that is able to photoreduce the central Rh atom by two electrons resulting in a Ru^{II}-Rh^{I}-Ru^{II} complex (Figure 1.6). This photoreduction is accompanied by a structural change at the central Rh atom in which the two chloride ligands are lost, and the geometry shifts from octahedral to square planer as shown in Figure 1.6.[58]

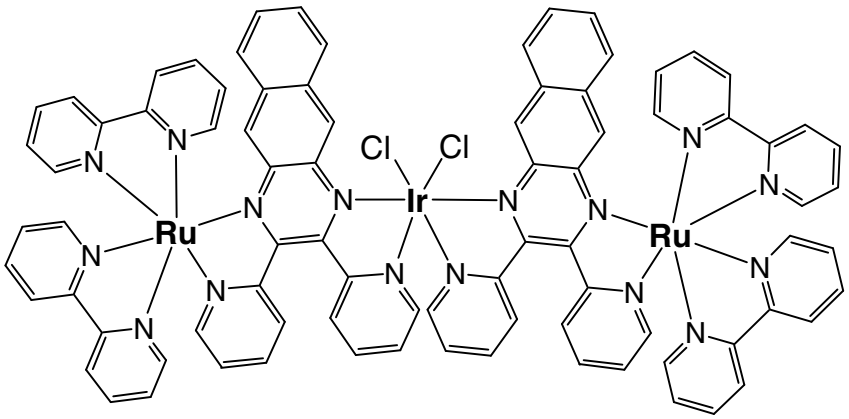

Figure 1.5 Ru^{II}-Ir^{III}-Ru^{II} trimer.

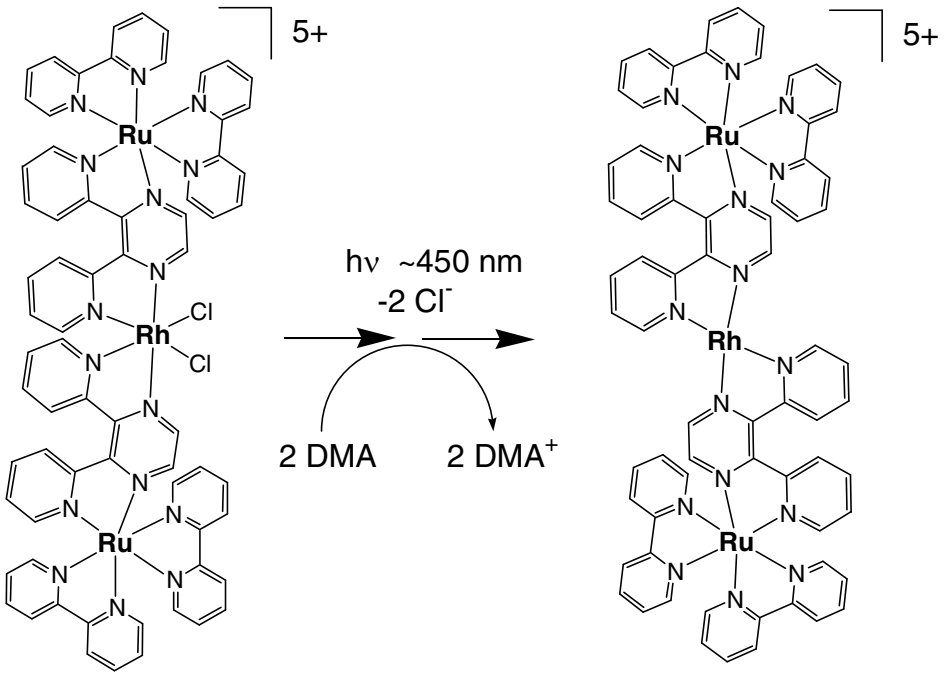

Figure 1.6 Photoreduction and structural shift in Ru^{II}-Rh^{III}-Ru^{II} trimer.

This lab developed two additional ruthenium (II) polypyridyl complexes capable of storing multiple electrons. These two complexes $[(phen)_2Ru(tatpp)Ru(phen)_2]^{4+}$ (**P**) complex and the $[(phen)_2Ru(tatpq)Ru(phen)_2]^{4+}$ (**Q**) are shown in Figure 1.7. **P** and **Q** have been shown to undergo photo driven 2 and 4 electron reductions, respectively, in both CH_3CN and water.[20,59,60] Under basic conditions, the photoreductions of both of these complexes appear as a series of one electron steps, but when the pH is lowered to 6-8, the central bridging ligands become protonated and the reductions merge to where only two electron steps are seen. The ability of the bridging ligands tatpp and tatpq to store multiple electrons seems to stem from weak electronic coupling between the bipyridine-like orbitals and the tetraazapentacene-like or quinone-like orbitals. This coupling allows

the initially populated bipyridine-like orbitals to undergo an intramolecular electron transfer, which reduces the central portion of the ligand. This ability to transfer the electron allows for subsequent reductions at the bipyridine-like orbital.[20,59,60]

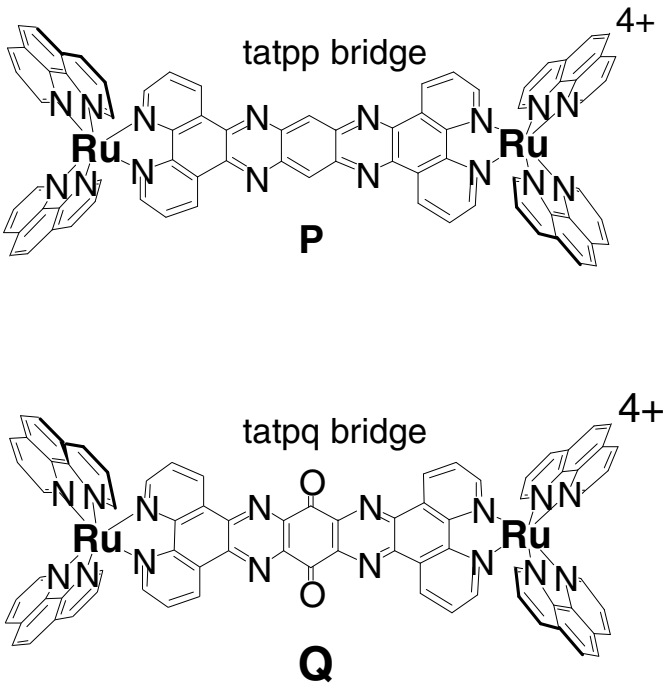

Figure 1.7 Ruthenium (II) polypyridyl complexes **P** and **Q**.

1.5 Scope of the Thesis

While the multi-electron reduction of complexes **P** and **Q** have been investigated in both acetonitrile and aqueous solvents at a variety of pH conditions, we have not yet explored the potential of these complexes to evolve H_2 and thus to establish their competency as potential photocatalysts for HER and ultimately in applications for the

WSR. Photoreduced **P** and **Q** should be able to easily meet the 2-electron requirement of the HER and thus the key questions are do they have the necessary energy to drive this reaction and how efficient are such photocatalysts compared to Rubpy and other related hydrogen evolving systems. It is clear that a co-catalyst is needed to release the H_2 'stored' within the photoreduced **P** and **Q**, and in this thesis we evaluate several co-catalysts and have worked to optimize conditions for H_2 evolution. In chapter 3, we report on the ability of **Q** and to a lesser extent **P** to drive the HER in acetonitrile under a variety of conditions. Figures of merit such as quantum yield and catalytic turnover numbers are reported and these data are analyzed with respect to other photocatalytic hydrogen evolving systems in the literature.

In chapter 2, we describe our efforts to develop microwave-assisted synthetic procedures for the photocatalyst **P**, and two related complexes: [(4,4'-bis(tert-butyl)-2,2'-bipyridine)$_2$Ru(tatpp)Ru(4,4'-bis(tert-butyl)-2,2'-bipyridine)$_2$]$^{4+}$ (**tP**) and [(4,4'-bis(tert-butyl)-2,2'-bipyridine)$_2$Ru(tatpq) Ru(4,4'-bis(tert-butyl)-2,2'-bipyridine)$_2$]$^{4+}$ (**tQ**). These complexes are needed in quantity for our photocatalytic studies and existing syntheses using simple thermal methods are often slow and low yielding. In this chapter, we explored the advantages and disadvantages of using microwave technology for such syntheses and report procedures, which are considerably faster than those previously known.

CHAPTER 2

MICROWAVE SYNTHESIS OF RUTHENIUM (II) POLYPYRIDYL COMPLEXES

2.1 Introduction

The advancement of supramolecular photochemistry has been greatly aided by understanding the photophysical properties of ruthenium (II) polypyridyl complexes, and how they function as photocatalysts. While the electrochemical and photochemical properties of complexes P and Q have been investigated,[20,59,60] there are numerous reasons to wish to prepare different derivatives in which the terminal or bridging ligands are modified. For example, replacement of the terminal bpy ligands to bpy ligands containing electron-withdrawing groups will raise the potential of the $Ru^{2+/3+}$ redox couple. Conversely, replacement with bpy ligands containing electron-donating groups tends to lower the potential of the $Ru^{2+/3+}$ redox couple. Other desirable effects are also possible through derivitization. Complexes containing 4,4'-di-t-butyl-2,2'-bipyridine tend to crystallize more readily and thus can be useful for X-ray crystallographic studies.

Unfortunately, the established synthetic procedure for **P** and **Q** [16] require long reaction times that makes the process slow and inefficient. As shown in scheme 2.1, the ligand substitution reaction between $[Ru(bpy)_2Cl_2]$ and tatpp requires a 7 days reflux to obtain P in 60% yield.

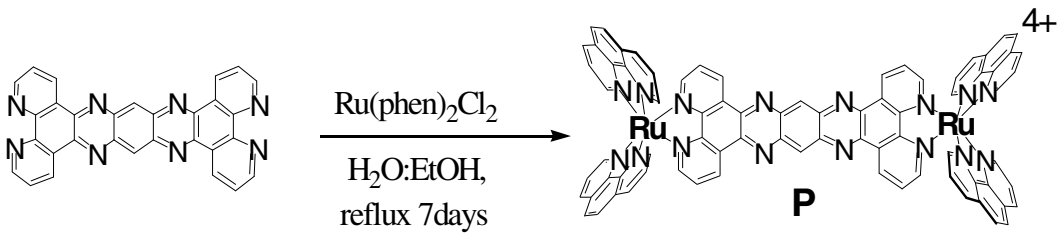

Scheme 2.1 Thermal synthesis of **P**.

Furthermore, these reaction conditions do not seem to be widely applicable and therefore the synthesis of each new derivative requires an optimization of the refluxing conditions and period for ligand substitution. With this ligand substitution step being the rate-determining factor within this multi-step synthesis, we decided to investigate microwaves-assisted synthetic procedures as this method has been shown in many cases to dramatically enhance reactions times and yields.

2.2 Microwave Assisted Synthesis

Progress in the field of microwave synthesis over the past 20 years has caused it to become a viable option as a means of decreasing reaction times within a wide range of syntheses. Traditional synthetic methods employ heat transfer equipment such as heating mantles, oil baths, or sand baths as a means of applying heat to a reaction. Since these methods first heat the reaction flask, a temperature gradient can develop within the reaction mixture leading to slow reaction times and possible degradation of the product or starting materials. Microwave dielectric heating is a process in which microwave energy is introduced remotely and directly heats the solvent and reactants resulting in a uniform

temperature increase in the reaction flask. This can result in less side products, less degradation, and shorter reaction times.

Microwaves are electromagnetic waves that are located between radio and infrared waves on the electromagnetic spectrum. These waves range from frequencies of 0.3 GHz to 300 GHz, but due to radar and telecommunication also operating in this range of frequencies, microwaves intended for heating are regulated to operate at 2.45 GHz, or a wavelength of 12.2 cm.[61-63] Microwave radiation consists of an electric field and a magnet field like all electromagnetic radiation. The characteristic dielectric heating that is indicative of microwave radiation is a result of its electric field interacting with dipoles or charged particles within the reaction mixture.[61]

There are two basic mechanisms through which microwaves are able to heat a given sample. The first of which is the dipolar polarization mechanism, in which the solvent or reactant must have a dipole moment in order to generate heat upon microwave irradiation. The oscillating electric field that microwaves possess cause a rotation in molecules with dipoles in an attempt to align with the electric field. The frequency of microwave radiation is low enough to allow dipoles ample time to react to the changing electric field and begin to rotate. The frequency is also high enough to insure the dipoles cannot synchronize with the changing electric field. This results in a phase difference in which energy is lost as heat through molecular friction and collisions.[62] It is important to choose an appropriate solvent when using microwave radiation. One intensive property that directly effects a solvents ability to be heated by microwaves is its dielectric constant, which is its ability to be polarized by an electric field.[63] The higher the

dielectric constant, the better it couples with microwave radiation. Examples of dielectric constant values are given in table 2.1.

Table 2.1 Dielectric Constants for Specific Solvents.

Solvent	Dielectric constant
Hexane	1.9
Carbon tetrachloride	2.2
Chloroform	4.8
Ethyl acetate	6.2
Methylene chloride	9.1
Acetone	20.6
Ethanol	24.6
Methanol	32.7
Acetonitrile	36
Dimethylformamide	36.7
Ethylene Glycol	41
Formic Acid	58
Water	80.4

The other mechanism through which microwaves are able to heat is the conductive mechanism. Under the influence of an electric field, charged particles within a solution will travel back and forth increasing the collision rate and releasing energy as heat.[62] These mechanisms allow for the rapid and uniform heating of reaction mixtures, which greatly improve the efficiency of many syntheses. The increase in yields and rates,

which accompany many microwave liquid phase reactions, is thought to be caused by superheating. This microwave specific effect allows some solvents to boil at 30°C above their normal boiling point.[64] These characteristics of microwave radiation are taken advantage of in many reactions in order to decrease reaction times along with side products and degradation that might occur over longer periods of heating.

There are numerous examples of enhanced syntheses by using microwaves.[61-63] Of particular interest here is the tremendous benefits seen in many ligand substitution reactions involving coordination compounds that have substitutionally-inert metal ions.[65] For example, the complex $[RuCl(CO)(bpy)_2]Cl$ can be synthesized from $RuCl_3$ and bpy by thermal heating for 168 hrs. By using microwave radiation, this same complex was synthesized in 70% yield after being heated for 1 minute (Scheme 2.2).[66]

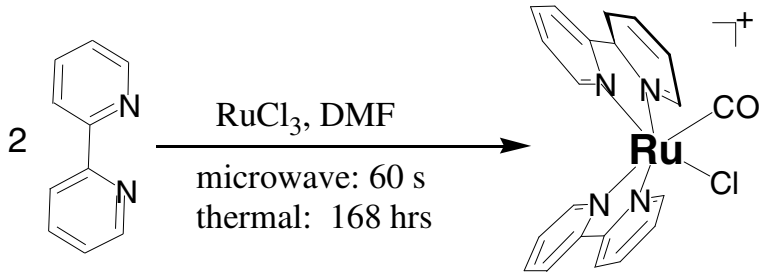

Scheme 2.2 Synthesis comparison of $Ru(bpy)_2CO(Cl)$.

Microwave radiation has become a viable choice in a wide range of chemical syntheses due to its large effect on reaction times and the enhanced purity of products that result in some cases. The microwave synthesis of Ru(4,4'-bis(tert-butyl)-2,2'-bipyridine)$_2Cl_2$ was able to decrease reaction time while increasing the overall purity of the synthesis. Refluxing 4,4'-bis(tert-butyl)-2,2'-bipyridine and $Ru(COD)Cl_2$ for 72 hrs

gave the desired product in a 78% yield, but microwave synthesis decreased the reaction time to 45 min and increased the purity to a 98% yield (Scheme 2.3).[67,68]

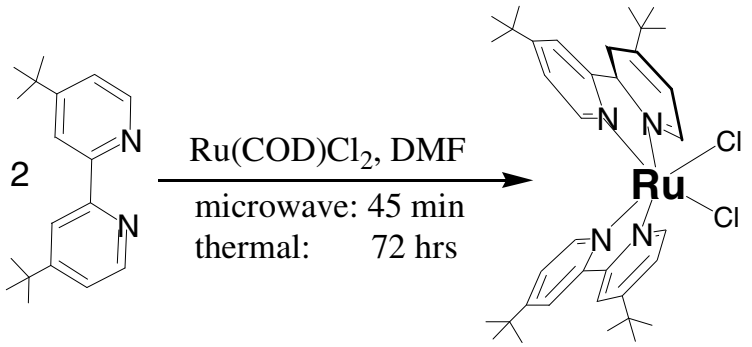

Scheme 2.3 Synthesis comparison of Ru(bis-t-butylbpy)$_2$Cl$_2$.

2.3 Experimental

2.3.1 Materials

Ethylene glycol (Aldrich), absolute ethanol (Aaper), acetonitrile (Aldrich), N,N-dimethylformamide (Aldrich), $RuCl_3$ hydrate (Pressure Chemical), cyclooctadiene (Aldrich), sodium amide (Aldrich), sodium persulfate (Aldrich), 4-t-butyl-pyridine (Aldrich), and 1,10-phenantroline (Alfa) were purchased and used without further purification. Ru(phen)$_2$Cl$_2$[69], tetraazatetrapyridopentacine (tatpp)[16], Ru(cyclooctadiene)Cl$_2$[70], 4,4'-bis(tert-butyl)-2,2'-bipyridine[71], and Ru(4,4'-bis(tert-butyl)-2,2'-bipyridine)$_2$Cl$_2$[67] were synthesized according known literature procedures.

2.3.2 Instrumentation

Microwave synthesis was performed in a CEM Microwave Sample Preparation System MDS-2000. This instrument has a maximum power of 630 Watts and can be programmed to operate at a given percentage of this value. The microwave oven was

fitted with a reflux condenser that passed through the top of the microwave cavity. Proper safety precautions were taken to ensure that there was no microwave leakage above the allowable limit.

^{1}H and ^{13}C NMR spectra were obtained on a JEOL Eclipse Plus 500 or 300 MHz spectrometer. Chemical shifts are given in ppm and are referenced to the residual proton signal from the deuterated solvent, being either MeCN-d^3 or acetone-d^6. UV-Vis data were obtained on a Hewlett Packard HP84535A spectrophotometer under the given conditions. ESI Mass Spectra were obtained on a Thermo Electron LCQ Deca-XP mass spectrometer. Elemental analyses were obtained on a Perkin Elmer PE2400 Series II CHN analyzer.

2.3.3 Synthesis

[(4,4'-bis(tert-butyl)-2,2'-bipyridine)$_2$Ru(tatpp)Ru(4,4'-bis(tert-butyl)-2,2'-bipyridine)$_2$](PF$_6$)$_4$ (**tP**)

A suspension of 0.120 g (0.247 mmol) tatpp in 120 mL ethanol and 120 mL water was first sonicated for 1 minute and then Ru(4,4'-bis(tert-butyl)-2,2'-bipyridine)$_2$Cl$_2$ (0.350 g, 0.494 mmol) and 2.5 mL concentrated HCl were added. The resulting mixture was heated in the microwave oven at 315 W for 5 hours during which the solution was observed to vigorously reflux. The reaction mixture was then cooled to RT and filtered through a pad of celite. The resulting filtrate was then concentrated by rotary evaporation to approximately 50% volume, during which a small precipitate forms (most likely starting material). This solid was removed by filtration. An aqueous NH_4PF_6 solution (50 mg/mL) was then added to the filtrate, which caused the product to precipitate. The

product was then filtered, washed with H_2O, and dried under vacuum at 60ºC. The crude product was purified by metathesis (interchanging PF_6^- and Cl^-). The product was dissolved in acetone and added to a solution of N-tetra-butyl ammonium chloride in acetone (50 mg/mL). The precipitant (Cl^- salt of **tP**) was then filtered out and dried under vacuum at 60ºC. The Cl^- salt was dissolved in H_2O and added to an aqueous NH_4PF_6 solution (50 mg/mL). The precipitant (PF_6^- salt of **tP**) was filtered out and dried under vacuum at 60ºC. Yield (PF_6^- salt): 0.219 g (38%). Anal. Calcd for **tP$(PF_6)_4 \cdot H_2O$,** $Ru_2C_{102}H_{112}N_{16}OP_4F_{24}$: C, 51.86; H, 4.70; N, 9.49. Found: C, 51.48; H, 4.77; N, 9.08. ^{1}H NMR (δ, 300MHz, acetone-d_6): 9.83 (d, J = 8.1 Hz, 4H), 9.68 (s, 2H), 8.95 (s, 4H), 8.93 (s, 4H), 8.51 (d, J = 4.8 Hz, 4H), 8.11(dd, J_1 = 8.1 Hz, J_2 = 5.4 Hz, 4H), 8.04(d, J = 6.3 Hz, 4H), 7.99 (d, J = 5.7 Hz, 4H), 7.65 (d, J = 5.7 Hz, 4H), 7.47 (d, J = 6.0 Hz, 4H), 1.44 (s, 36H), 1.36 (s, 36H). ^{13}C NMR (δ, 500 MHz, MeCN-d_3): 162.99, 162.85, 157.12, 156.89, 154.34, 152.14, 151.62, 151.15, 143.07, 141.44, 133.72, 130.92, 130.56, 127.97, 124.86, 124.67, 121.77, 121.70, 35.49, 35.39, 29.64, 29.55.

[(4,4'-bis(tert-butyl)-2,2'-bipyridine)$_2$Ru(tetraazatetrapyridopentacenequinone) Ru(4,4'-bis(tert-butyl)-2,2'-bipyridine)$_2$]$(PF_6)_4$ (**tQ**)

A solution of 0.070 g (30 μmol) **tP** in 20 mL CH_3CN was prepared along with a solution of 0.042 g (0.18 mmol) sodium persulfate in 17 mL DI water. The two solutions were combined and refluxed for 6 hours. The acetonitrile was removed by rotary evaporation, which caused the product to precipitate. The product was then filtered out, washed with H_2O, and dried under vacuum at 60ºC. Yield (PF_6^- salt): 0.0475 g (67%). Anal. Calcd for **tQ**$(PF_6)_4 \cdot 2H_2O$ $Ru_2C_{102}H_{112}N_{16}O_4P_4F_{24}$: C, 50.83; H, 4.52; N, 9.30.

Found: C, 51.02; H, 4.90; N, 8.48. ^{1}H NMR (δ, 300MHz, MeCN-d_3): 9.71 (d, J = 8.1 Hz, 4H), 8.55 (s, 4H), 8.51 (s, 4H), 8.30 (d, J = 5.1 Hz, 4H), 8.02 (dd, J_1 = 8.1 Hz, J_2 =5.1 Hz, 4H), 7.70 (d, J = 6.0, 4H), 7.59 (d, J = 6.0, 4H), 7.50 (d, J = 5.7, 4H), 7.24 (d, J = 6.3, 4H), 1.46 (s, 36H), 1.36 (s, 36H).

$[(phen)_2Ru(tatpp)Ru(phen)_2](PF_6)_4$ (**P**)

A suspension of 0.20 g (0.41 mmol) tatpp and 40 mL ethylene glycol with 2 mL DI water was sonicated for 1 minute and heated in the microwave at 252 W for 2 minutes. Then 0.46 g (0.86 mmol) $Ru(phen)_2Cl_2$ was added and the solution was heated in the microwave 130 s at 630 W and then allowed to cool for 10 min. The solution was microwaved again for 130 s at 630 W and then allowed to cool for 10 min. This heating and cooling procedure was repeated a third time, after which 50 mL DI water was added to the solution and the resulting solution was thoroughly mixed. The solution was then filtered through a pad of celite to remove any unreacted tatpp. An aqueous NH_4PF_6 solution (70 mg/mL) was added to the filtrate to precipitate the product. It was then filtered, washed with H_2O, and dried under vacuum at 60ºC. The crude product was purified by one metathesis. The product was dissolved in acetone and added to a solution of N-tetra-butyl ammonium chloride in acetone (50 mg/mL). The precipitant (Cl^- salt of **tP**) was then filtered out and dried under vacuum at 60ºC. The Cl^- salt was dissolved in H_2O and added to an aqueous NH_4PF_6 solution (50 mg/mL). The precipitant (PF_6^- salt of **tP**) was filtered out and dried under vacuum at 60ºC. Yield 0.68 g (PF_6^- salt): 42%. This compound is identical to that reported in the literature.[16]

2.4 Results and Discussion

*2.4.1 Microwave Synthesis of **P***

The synthesis of $[(phen)_2Ru(tatpp)Ru(phen)_2]^{4+}$ (**P**) by refluxing the free tatpp ligand with a slight excess of $Ru(phen)_2Cl_2$ (Scheme 2.4) required long reflux periods in order to obtain decent yields (e.g. 60% yield). Our initial investigation using microwave-assisted syntheses focused on improving both the yields and time efficiency of this reaction. By using microwave radiation, the amount of time to carry out the coordination step in similar syntheses has been greatly reduced.[65,72]

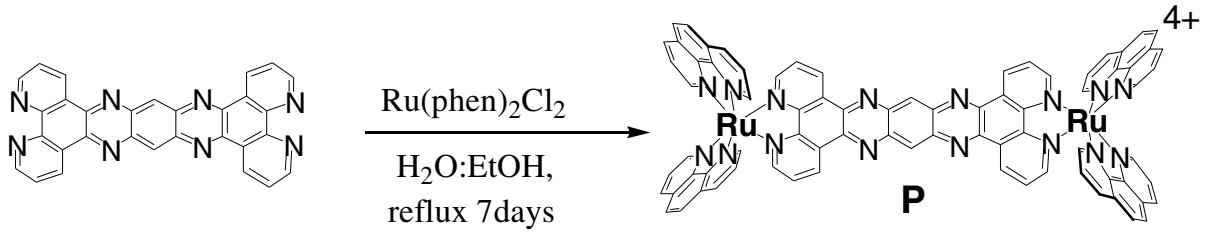

Scheme 2.4 Thermal synthesis of **P**.

Microwave-assisted syntheses with coordination compounds generally fall into one of two categories. Either the reaction solution is heated for short periods of time (1 – 5 min) at high power (500 –700W), or it is heated for much longer periods (hours) at lower power (250 – 400W). When heating at high power, solvents with high boiling points such as DMF and ethylene glycol are typically used due to the extreme conditions. Both of these methods were investigated in the synthesis of **P** with the syntheses conducted under high power and short reaction times ultimately proving superior.

The following two reactions highlight the differences seen between the two methods. Microwaving a suspension of $Ru(phen)_2Cl_2$ and tatpp in 50:50 water: ethanol

at 315 W for 5 h ultimately yielded a product that showed more impurities and required a significantly longer reaction time (Table 2.2). Conversely, short microwaving periods of 130 s at 630 W yielded a cleaner product, however, the heating process had to be repeated at least 3 times to optimize the yield. The solution was allowed to cool for 10 min between each heating period in order to avoid over heating and product degradation. Other important details are the sonication step and initial microwave irradiation step for the ethylene glycol tatpp mixture. These steps are done to help solubilize the tatpp ligand before the $Ru(phen)_2Cl_2$ is added. The $Ru(phen)_2Cl_2$ was then added to the reaction mixture and refluxed over various periods of time to determine the optimum reaction time for this synthesis. In each attempted synthesis, the reaction mixture was heated for 130 s, allowed to cool, then repeated for a given number of cycles. This synthesis was carried out while heating it for 2 cycles, 3 cycles, 4 cycles, and 6 cycles, which resulted in total reaction times of 260 s, 390 s, 520 s, and 780 s respectively (Table 2.2).

Table 2.2. Approximate Amounts of P in the Crude Yield of Various Reactions.

Reaction time	**Power (W)**	**Solvent**	**% Crude Yield**	**% P**
260 s	630	ethylene glycol	40	70
390 s	630	ethylene glycol	50	95
780 s	630	ethylene glycol	50	95
5 hrs	315	EtOH:H_2O	60	85
7 days	Thermal	EtOH:H_2O	85	70

Heating the reaction mixture for 3 cycles (390 s) proved to be the cleaner and more efficient synthesis. The reaction was also carried out in which only half of the $Ru(phen)_2Cl_2$ was added and heated for 3 cycles, then the other half was added and heated for 3 more cycles. This was not successful in increasing the purity or quantity of the desired product. It was also found that the $Ru(phen)_2Cl_2$ starting material must be freshly prepared otherwise the reaction results in mostly side products and starting materials. No $Ru(phen)_2Cl_2$ over 2 weeks old should be used in this reaction. Ultimately, the best microwave-assisted syntheses found was that as indicated in scheme 2.5 in which tatpp and $Ru(phen)_2Cl_2$ in ethylene glycol : water (20:1) are irradiated with microwaves at 630 W for 3 cycles of 130 s and allowed to cool between cycles. This does not yield a pure product, however, the work-up is relatively simple and one set of metathesis reactions give the pure complex in 42% overall yield from tatpp.

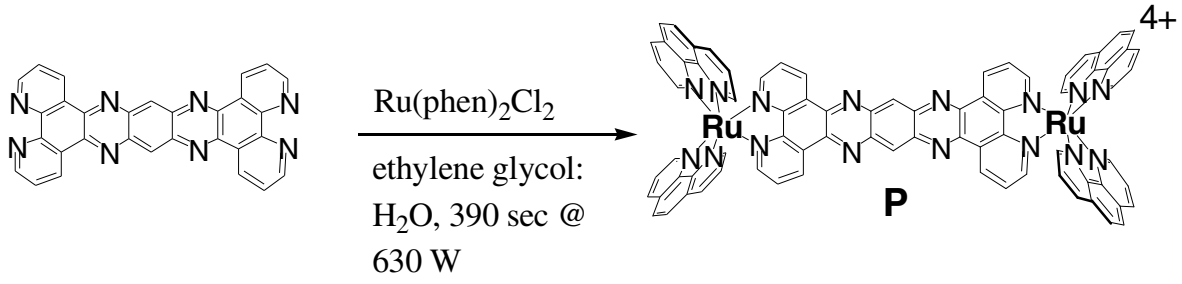

Scheme 2.5 Microwave synthesis of **P**.

The reported thermal synthesis of complex **P** requires 7 days of reflux with a % yield of 50% – 65%. The crude product in the thermal synthesis is much dirtier than what is found in the microwave synthesis. The range of % yields for the thermal process is due to the number of times a metathesis (interchanging Cl^- and PF_6^-) must be done to

purify the product. The thermal product requires 4–5 metatheses depending on the purity of the crude product, while the microwave product only requires 1 metathesis. Not only has the reaction time been reduced from 7 days to $6^1/_2$ min, but the amount of time used to clean the crude product has also been significantly lowered. The decrease in overall % yield is the only set back to the microwave synthesis, but considering the vast improvements that have been made with respect to reaction time; the microwave synthesis is the preferred method.

2.4.2 Microwave Synthesis of Ru(4,4'-bis(tert-butyl)-2,2'-bipyridine)$_2$Cl$_2$

A known procedure was followed in this synthesis,[67] but other synthetic methods were explored as a means of comparison. A thermal procedure was attempted similar to that used in the synthesis of Ru(phen)$_2$Cl$_2$. Ru(II)Cl$_3$ and 4,4'-bis(tert-butyl)-2,2'-bipyridine were refluxed in dry DMF for 5 hrs. This resulted in mostly starting material. This synthesis was also attempted under the conditions that were most successful in the synthesis of complex **P**. Ru(cod)Cl$_2$ and 4,4'-bis(tert-butyl)-2,2'-bipyridine in ethylene glycol and water were heated for 3 cycles of 130 s at 630 W in the microwave. This resulted in what appeared to be Ru(4,4'-bis(tert-butyl)-2,2'-bipyridine)$_3^{2+}$. This would be a quick and viable means of synthesizing Ru(4,4'-bis(tert-butyl)-2,2'-bipyridine)$_3^{2+}$, but it was not further investigated here since it was not the desired product. The reported microwave synthesis for Ru(4,4'-bis(tert-butyl)-2,2'-bipyridine)$_2$Cl$_2$ calls for Ru(cod)Cl$_2$ and 4,4'-bis(tert-butyl)-2,2'-bipyridine in dry DMF to be heated under approximately 300 W of microwave radiation for 45 min, which resulted in a 60% yield (Scheme 2.6).

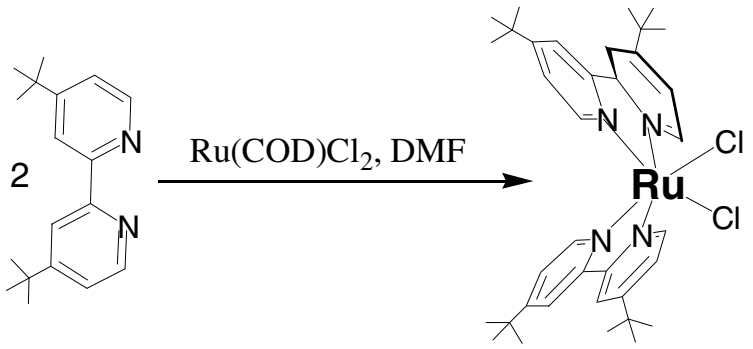

Scheme 2.6 Synthesis of Ru(bis-t-butylbpy)$_2$Cl$_2$.

2.4.3 Microwave Synthesis of tP

The development of a viable microwave assisted synthesis of complex **tP** involved a number of different reactions with various results. Each reaction involved the coordination of Ru(4,4'-bis(tert-butyl)-2,2'-bipyridine)$_2$Cl$_2$ with tatpp. Under the first set of conditions, the reaction mixture was heated under microwave radiation of 630 W for 130 s intervals in which it was allowed to cool for 10 min between each heating period in order to avoid over heating and product degradation. For each reaction, the tatpp was first suspended in the ethylene glycol: water mixture, sonicated, and then heated in the microwave to help solubilize the bridging ligand. The Ru(4,4'-bis(tert-butyl)-2,2'-bipyridine)$_2$Cl$_2$ was then added to the reaction mixture and heated for a given number of 130 s cycles. When heated for 3 cycles (390 s), consisted of equal amounts of the dimer **tP,** the mono product [(4,4'-bis(tert-butyl)-2,2'-bipyridine)$_2$Ru(tatpp)]$^{2+}$, and an unidentified side product. Since the desired product was being formed, the reaction time was increased to push the product distribution towards **tP**. This synthesis was carried out

while heating it for 5 cycles, 6 cycles, 9 cycles, 12 cycles, and 18 cycles, which resulted in total reaction times of 650s, 780 s, 1170 s, 1560 s, and 2340 s respectively (Table 2.3).

Table 2.3 Approximate Product % in the Crude Yield of Microwave Reactions at 630W.

Reaction time	**% Crude Yield**	**% tP**	**% monomer**	**% side product**
390 s	90	20	40	40
650 s	90	10	45	45
1170 s	90	5	45	50
1560 s	110	1	50	49
2340 s	110	0	50	50

It was found that as the reaction time increased, the product distribution shifted towards the mono product. The reaction that was heated for 9 cycles resulted in a crude product that was approximately 45% mono product, 50% side product, and 5% **tP**. Heating the reaction mixture for longer than 9 cycles resulted in essentially the same product with no trace of **tP**. The crude product from the 1170 s reaction was eluted through a short plug of silica gel with CH_3CN, and successfully separated **tP** from the mono product, but the side product would not separate even when it was attempted with longer columns. Since this method was clearly favoring the mono product, a reaction mixture that had been heated for 9 cycles was taken and mixed with more Ru(4,4'-bis(tert-butyl)-2,2'-bipyridine)$_2Cl_2$ and heated for $2^1/_2$ hrs at 315 W in an attempt to push the reaction towards the desired product **tP**. This was not successful in producing more of the dimer. This method of heating for short periods of time at high power did not prove to be a viable means of synthesis for **tP**, but it does show promise in synthesizing the mono product $[(4,4'\text{-bis(tert-butyl)-2,2'-bipyridine})_2Ru(tatpp)]^{2+}$. However, the side

product formed in this reaction would not separate from this product and thus poses a potential problem in continuing this synthesis. Since the mono product was not the goal, it was not investigated any farther than this.

The microwave reaction conditions for this synthesis were then adjusted to heat the reaction mixture at a lower power for a longer period of time. For each reaction, the tatpp was first suspended in a 50:50 water: ethanol solution and sonicated. The Ru(4,4'-bis(tert-butyl)-2,2'-bipyridine)$_2$Cl$_2$ was then added and heated by microwave radiation for a given amount of time. In the first attempt of this method, the reaction mixture was heated at 252 W for 1 hr and resulted in a cleaner product that had a larger percentage of **tP** than the mono product. When run for longer periods of time at 315 W, the product distribution shifted greatly towards **tP**, which can be seen in table 2.4.

Table 2.4 Approximate Product % in the Crude Yield
During the Synthesis of **tP.**

Reaction time	**% Crude Yield**	**% tP**	**% monomer**	**% side product**	C_{HCl}
1 hr	100	40	30	30	-
3 hrs	100	33	33	33	-
4 hrs	60	70	15	15	0.13 M
5hrs	40	100	0	0	0.13 M
7 days	110	10	45	45	-

In the initial attempts, this synthesis was still producing the same side product that could not be removed from the high power synthesis. This side product was assumed to be a bridged species containing two Ru(4,4'-bis(tert-butyl)-2,2'-bipyridine)$_2$Cl$_2$ molecules that were possibly connected by water molecules. In an attempt to keep this side product from forming, concentrated HCl was added which would cause this bridged

species to dissociate. Two interesting things occurred once HCl was added to the reaction mixture: 1) The side product was no longer being formed, and 2) the unreacted Ru(4,4'-bis(tert-butyl)-2,2'-bipyridine)$_2$Cl$_2$ starting material would precipitate from the solution once the ethanol was removed by rotary evaporation. This greatly increased the purity of the crude product. It was also found that the recovered unreacted Ru(4,4'-bis(tert-butyl)-2,2'-bipyridine)$_2$Cl$_2$ could be reused in the reaction and resulted in a cleaner crude product.

Using this procedure, the reaction mixture was heated for various times at 315 W and found to be the most effective when reacted for 5 hrs. The reaction of Ru(4,4'-bis(tert-butyl)-2,2'-bipyridine)$_2$Cl$_2$ with tatpp in an acidic water: ethanol solution produced **tP** in a 38% yield (Scheme 2.7).

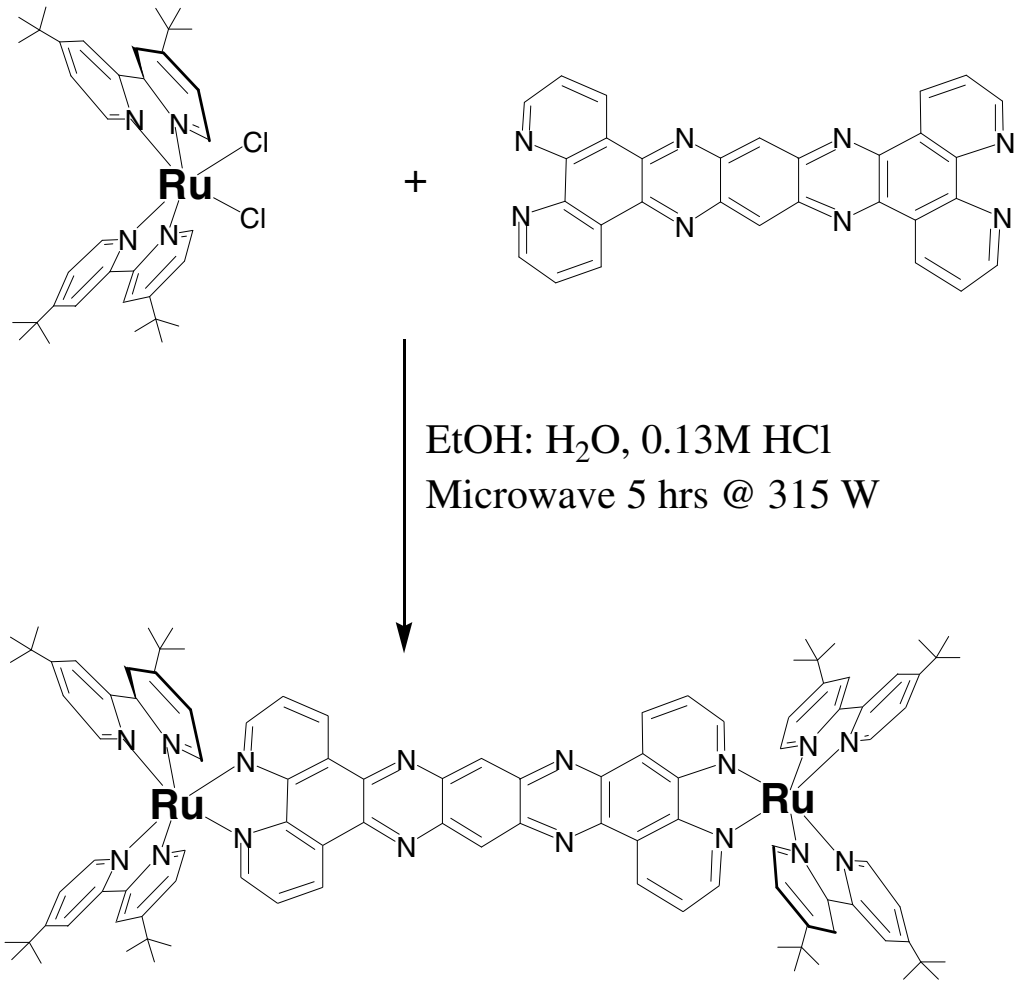

Scheme 2.7 Microwave synthesis of **tP.**

The complex **tP** was characterized by elemental analysis, ESI-MS, ^{1}H NMR, ^{13}C NMR, and COSY NMR spectroscopy. The ^{1}H NMR spectrum (Figure 2.1) was assigned with the aid of COSY analysis and by comparison with the spectrum of complex **P**. The ESI-MS spectrum for complex tP (Figure 2.2) indicates an apparent aggregation of this complex. M represents one **tP** molecule in which a given number of PF_6^- anions have been removed leaving the molecule with an overall net charge. The four major peaks

expected for **tP** can be clearly seen at 441.5, 636.13, 1026.75, and 2196.5 being the +4, +3, +2, and + charged **tP** molecules, respectively. A number of other peaks in the spectra have been identified as multiple molecules with their respective charge. It is believed that the **tP** molecules are aggregating through a π-π stacking mechanism of the central bridging ligands. The UV-VIS spectrum of **tP** can be found in Appendix A.

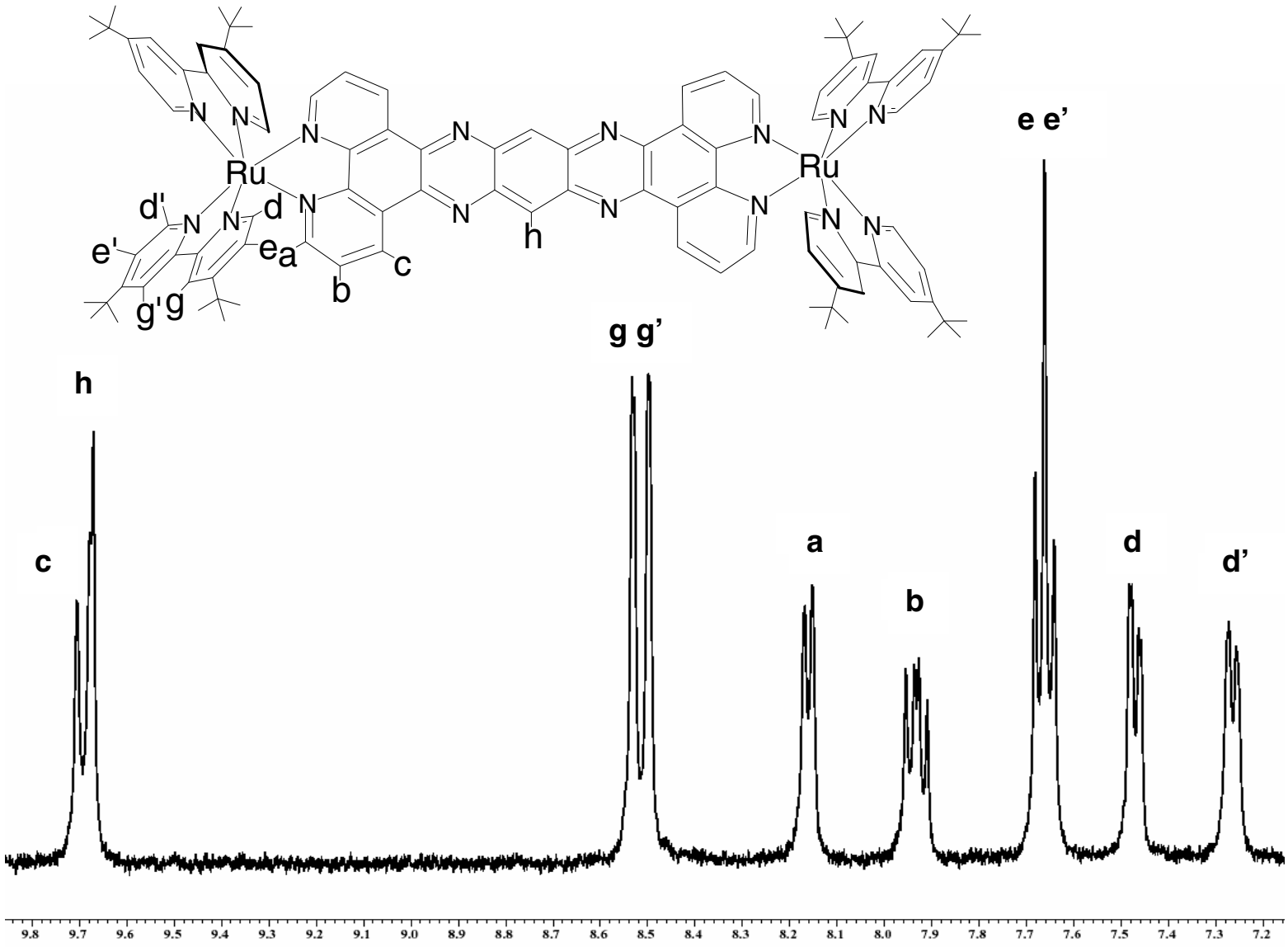

Figure 2.1 Partial ^{1}H NMR of **tP**

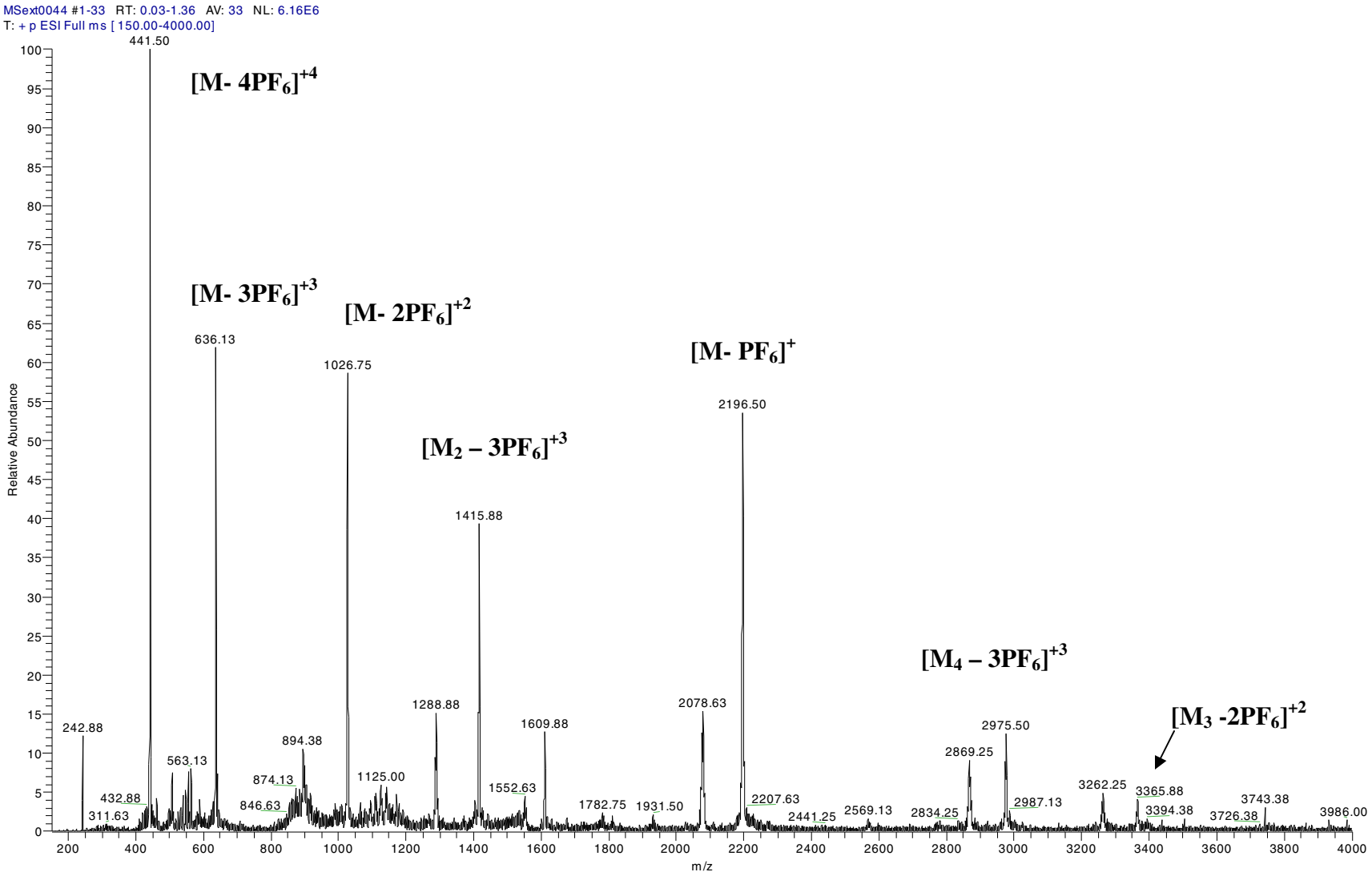

Figure 2.2 ESI-MS of **tP**

The thermal synthesis of **tP** was also attempted as a means of comparison. Ru(4,4'-bis(tert-butyl)-2,2'-bipyridine)$_2$Cl$_2$ and tatpp in a solution of 50:50 water: ethanol was refluxed for 7 days. This reaction resulted in a very impure crude product and showed no signs of being better than the microwave synthesis. Since adding acid to the reaction mixture in the second microwave synthesis was successful in removing the side product, the same thing was tried in the method that resulted in the mono product [(4,4'-bis(tert-butyl)-2,2'-bipyridine)$_2$Ru(tatpp)]$^{2+}$. This was not successful in removing the side product from this reaction.

2.4.4 Synthesis of tQ

The synthesis of **tQ** was achieved by a simple oxidation of **tP**. The complex **tP** was dissolved in CH_3CN while the oxidizing agent sodium persulfate was dissolved in water. These solutions were mixed and refluxed for 6 hrs. This resulted in the desired product in a 67% yield (Scheme 2.8).

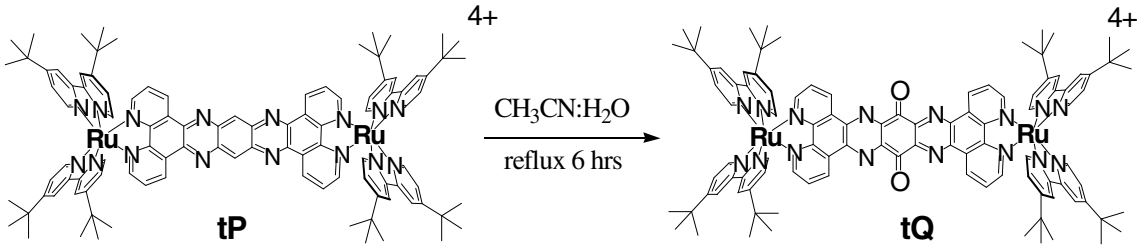

Scheme 2.8 Synthesis of **tQ**.

The complex **tQ** was characterized by elemental analysis, ESI-MS, ^{1}H NMR, and COSY NMR spectroscopy. The ^{1}H NMR spectrum (Figure 2.3) was assigned with the aid of COSY analysis and by comparison with the spectrum of complex **tP**. The ESI-MS spectra for complex **tQ** (Figure 2.4) indicates an apparent aggregation of this complex.

M represents one **tQ** molecule in which a given number of PF_6^- anions have been removed leaving the molecule with an overall net charge. The four major peaks expected for **tQ** can be clearly seen at 448.75, 1041.5, and 2227.13 being the +4, +2, and + charged **tQ** molecules, respectively. A number of other peaks in the spectra have been identified as multiple molecules with their respective charge. It is believed that the **tQ** molecules are aggregating through a π-π stacking mechanism of the central bridging ligands. The UV-VIS spectrum of **tQ** can be found in Appendix A.

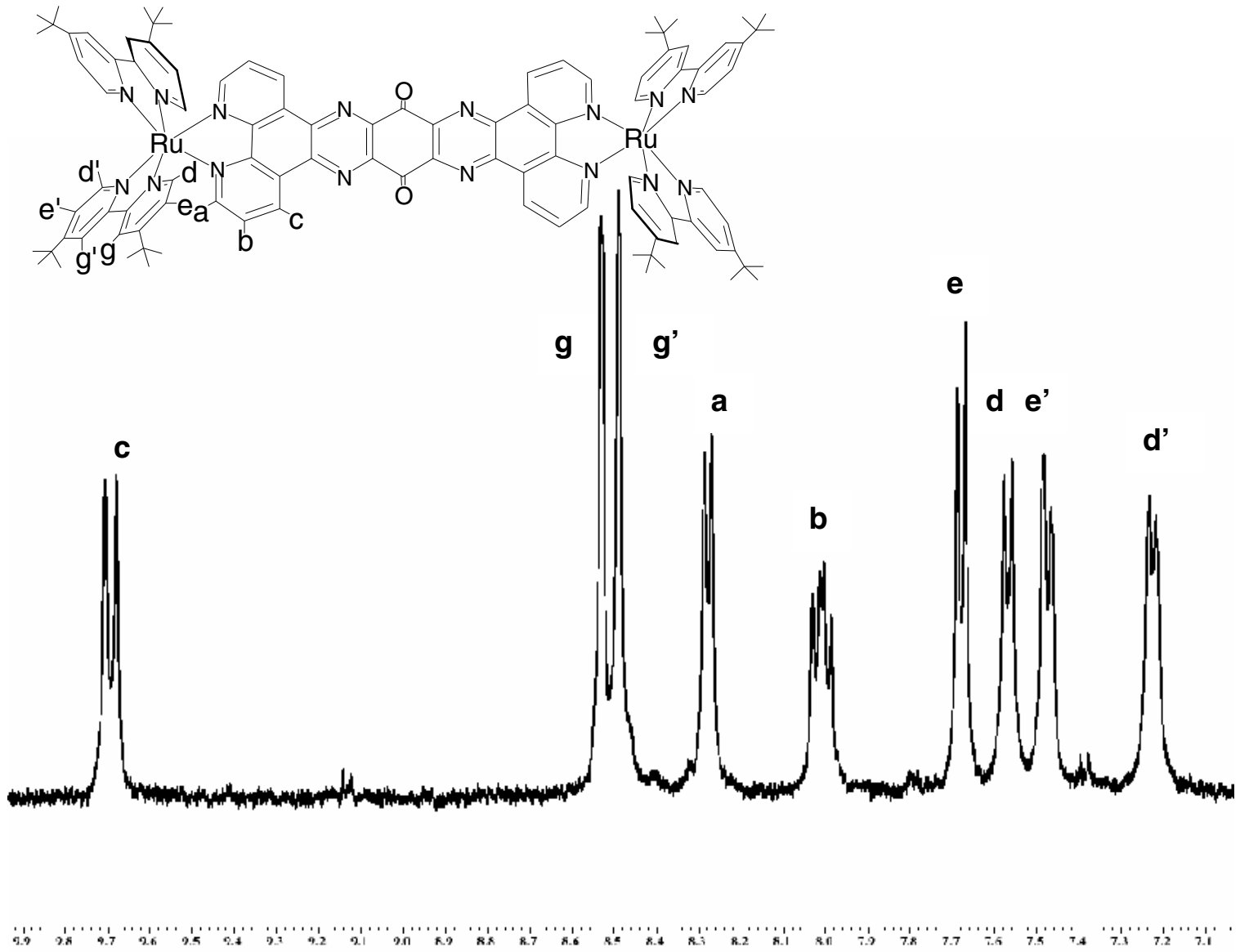

Figure 2.3 Partial ^{1}H NMR **tQ**

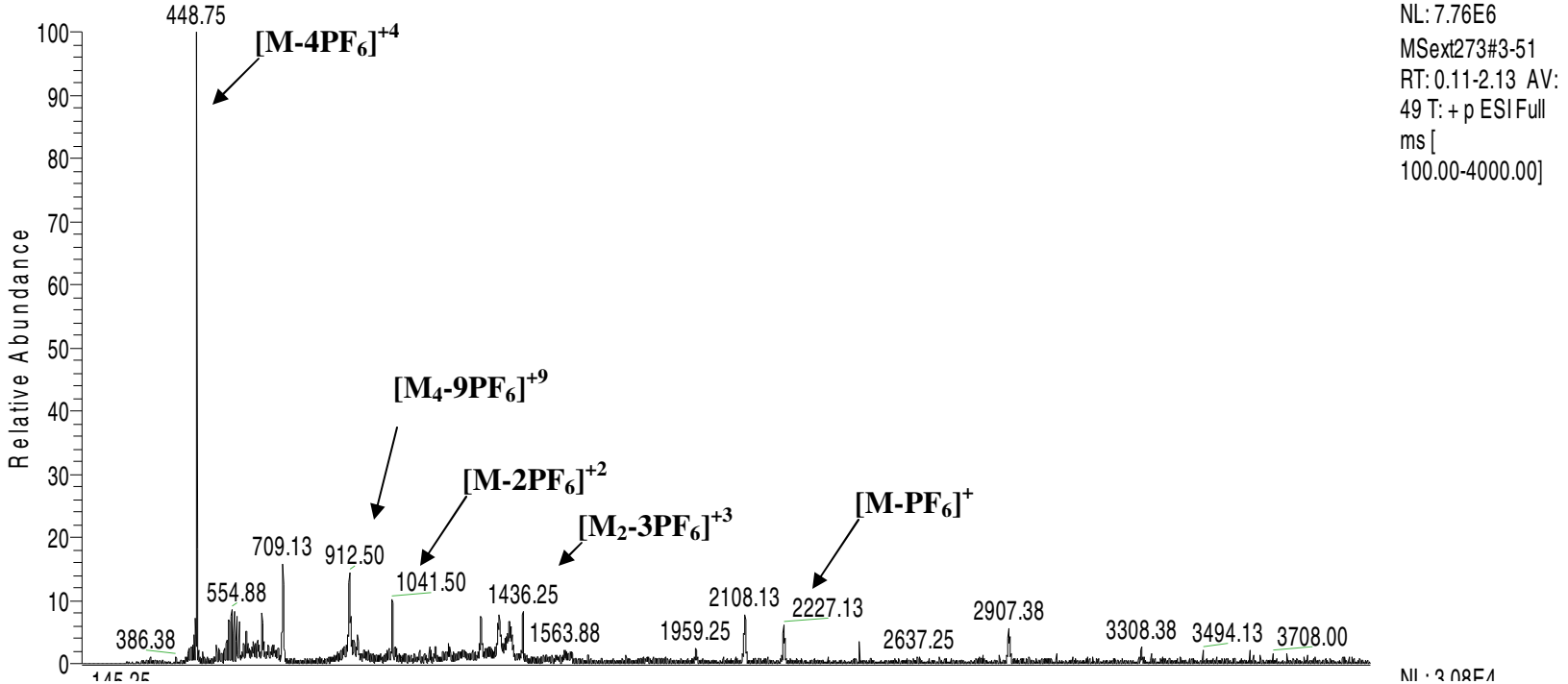

Figure 2.4 ESI-MS of **tQ**

2.5 Conclusion

This work shows the viability of microwave assisted synthesis within this family of complexes. The time dependent coordination step of tatpp with the ruthenium based molecules was significantly decreased, and a new method of synthesis has been established for complex **P.** The different microwave methods used to synthesize **P,** Ru(4,4'-bis(tert-butyl)-2,2'-bipyridine)$_2$Cl$_2$, and **tP** provide a starting point for the synthesis of similar complexes. The microwave synthesis was better than the thermal synthesis in each case due to the much lower reaction times and the increased purity of the crude products.

CHAPTER 3

PHOTOCATALYTIC HYDROGEN GENERATION FROM RUTHENIUM (II) POLYPYRIDYL COMPLEXES CONTAINING MULTI-ELECTRON ACCEPTOR LIGANDS

3.1 Introduction

With the ever-increasing need for alternant energy sources, more and more effort is being placed behind finding a viable means of utilizing solar energy. Nature itself provides the blueprint for light energy conversion within photosynthesis. This system's ability to transiently store light energy as high-energy molecules (ATP) and reducing potentials (NADH) makes it a valuable system to mimic. The mechanistic pathway in which this system converts H_2O into O_2 and CO_2 into glucose is highly complex. For that reason, most photosynthetic biomimetics take place on the molecular level and exploit the principles of energy conversion found in photosynthesis. The most basic need for a molecular system to mimic photosynthesis is a light harvesting chromaphore that utilizes solar energy to drive the process.

Ruthenium (II) polypyridyl complexes have acted as an integral part in the advancement of supramolecular photochemistry. These chromaphores have been used in numerous applications of solar energy conversion due to their propitious photochemical behavior.[27,37-41,73] $[Ru(bpy)_3]^{2+}$ is the standard photocatalyst from this group of compounds, whose discovery and subsequent photochemical studies have laid the groundwork for the use of metal to ligand charge transfer (MLCT) states in light to energy conversion.[12] The ^{3}MLCT state of the photoexcited $[Ru(bpy)_3]^{2+}$ complex is a

powerful redox agent which can act as a one electron oxidant or a one electron reductant (Figure 3.1).[12]

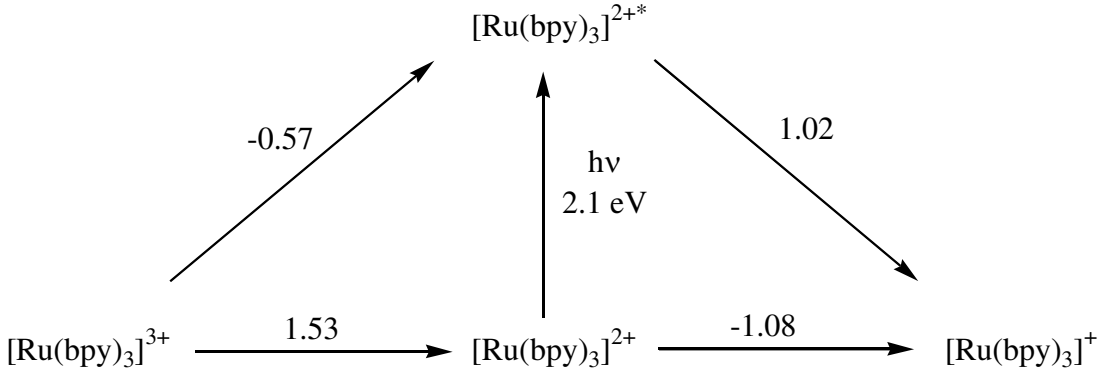

Figure 3.1 Photoexcited states of $[Ru(bpy)_3]^{2+}$.

The viability of $[Ru(bpy)_3]^{2+}$ as a photocatalyst is limited to one electron processes. This impedes its ability to be used as a photocatalyst in multi-electron processes necessary to mimic photosynthesis such as the hydrogen evolving reaction (HER) and the oxygen evolving reaction (OER).[26] Another short coming of $[Ru(bpy)_3]^{2+}$

$$2H^+ + 2e^- \rightarrow H_2 \qquad \text{Eq 3.1 (HER)}$$

$$2H_2O \rightarrow 4H^+ + 4e^- + O_2 \qquad \text{Eq 3.2 (OER)}$$

as a photocatalyst is its sensitivity to photochemical degradation by photolabilization of its ligands as the MLCT bands are excited.[74,75] The effectiveness of many photocatalyst is limited by these same issues. Only a small number of molecular photocatalyst with the ability to store multiple electrons have been reported,[20,76,77] and most systems are hampered by the instability of the reduced photocatalyst leading to a loss of catalytic function.

A class of long-lived dinuclear Ruthenium (II) photocatalyst with the ability to store multiple electrons is reported herein. The complexes $[(phen)_2Ru(tatpp)Ru(phen)_2]^{4+}$

($\mathbf{P^{4+}}$) and $[(phen)_2Ru(tatpq)Ru(phen)_2]^{4+}$ ($\mathbf{Q^{4+}}$) have the ability to reversibly store two or four electrons, respectively, upon photo irradiation in the presence of a sacrificial reducing agent (Figure 3.2).[16] The central bridging ligands, tatpp and tatpq, act as the sites for multi-electron storage. These unique photocatalysts not only have the ability to meet the multi-electron requirements of important small molecule activation reactions, like the hydrogen evolving reaction (HER), but they have also been shown to be photoactive for up to 9 days.

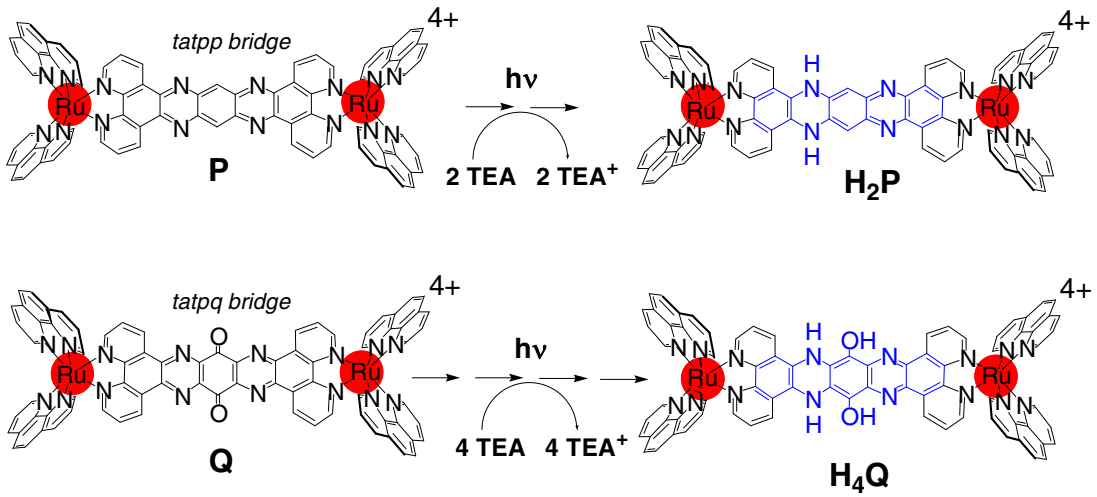

Figure 3.2 Photoreduction of **P** and **Q.**

A few similar Ruthenium polypyridyl photocatalyst have been recently reported in the literature. Brewer et al. has reported a trimeric Ru^{II}-Rh^{III}-Ru^{II} complex (Figure 3.3) in which the Rh^{III} center is photoreduced to give the Ru^{II}-Rh^{I}-Ru^{II} complex.[58] The doubly reduced structurally altered Rh^{I} site provides an accessible catalytic site for H_2 evolution. This complex in a CH_3CN and H_2O mixture (6:1) was able to produce H_2 in the presence of the sacrificial reducing agent DMA. A heterodinuclear Ru-Pd complex (Figure 3.4) has been reported by Rau et al. as another possible photocatalyst for the efficient

production of hydrogen.[78] In this complex, the photoactive Ru^{II} center acts as the light absorber, while the bridging ligand is used as an electron relay to the Pd catalytic center. A turnover number (TON) of 56.4 was reported for this complex under optimized conditions in a CH_3CN solution using TEA as the sacrificial reducing agent. A $[Ru(bpy)_3]^{2+}$, $Pt(II)Cl_2$ complex (Figure 3.5) reported by Sakai et al. has been reported to evolve H_2 from an aqueous EDTA, acetate buffer solution.[79] By combining the known photocatalytic abilities of these two catalysts, H_2 was evolved with a TON of 4.8. Even though little H_2 was produced, the significant result is that this complex was able to photochemically evolve H_2 from water. All three of these photocatalysts are similar to $[Ru(bpy)_3]^{2+}$ in the fact that they readily photodecompose due to the instability of their reduced species. Rau reports a cease of H_2 production at 30 h, while Sakai reports data up to 10 h.

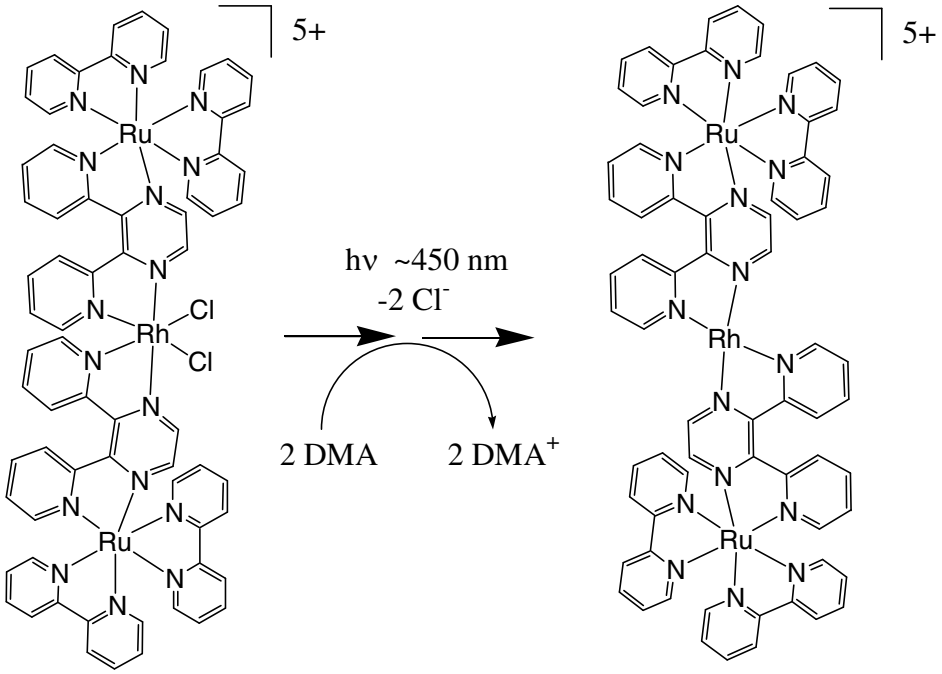

Figure 3.3 Reduction of a trimeric Ru^{II}-Rh^{III}-Ru^{II} complex.

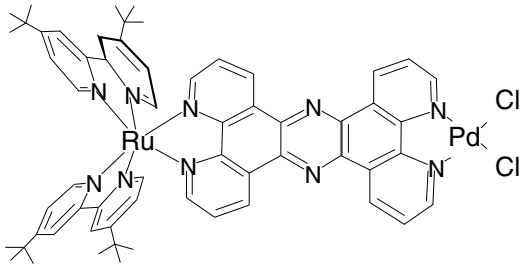

Figure 3.4 Heterodinuclear Ru-Pd complex.

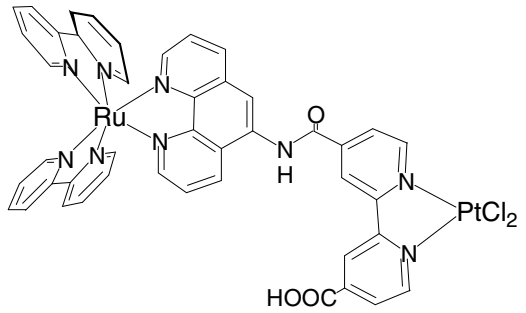

Figure 3.5 $[Ru(bpy)_3]^{2+}$, $Pt(II)Cl_2$ complex.

3.2 Experimental

3.2.1 Materials

Acetonitrile (Aldrich), triethylamine (Aldrich), hexafluorophosphoric acid (Aldrich), sulfuric acid, 1,10-phenanthroline (Alfa), 2,2'-bipyridine (Alfa), potassium tris(oxalato)ferrate(III) trihydrate (Strem), sodium propionate (Alfa), $Pd(bpy)Cl_2$ (Aldrich), $Pt(bpy)Cl_2$ (Aldrich), and $NiCl_2$ (Aldrich) were purchased and used without further purification. $Ru(bpy)_3^{2+}$, P, and Q were synthesized according to known literature procedures.[16] Triethylammonium hexafluorophosphate ($TEAHPF_6$) was prepared by slow addition of 20 mL of TEA (0.14 mol) to 75 mL of a cooled aqueous solution containing 50 g (0.34 mmol) hexafluorophosphoric acid with stirring. A white

precipitant formed which was then filtered out and dried under vacuum at 60ºC. Yield 19 g (55%).

3.2.2 Instrumentation

UV-Vis data were obtained on a Hewlett Packard HP84535A spectrophotometer under the given conditions.

3.2.3 Photoreactor Setup

Photochemical reactions were performed in one of two photochemical reactors consisting of Ace Glass model 7840 reactors with total volumes of approximately 400 mL (Figure 3.6). A water-cooled jacket between the light source and solution maintains a constant temperature of 21ºC. The solution volumes of 315 mL and 250 mL for photoreactors 1 (PR1) and 2 (PR2), respectively, were set to ensure that the solution level was above the top of the light source. The light path length within the photoreactor is 1.55 cm. Our light source consists of 64 Kingbright T-$1^3/_4$ (5mm) Round LEDs, which have a peak wavelength of 467 nm and a spectral line half-width of 30 nm. All samples were deoxygenated by bubbling N_2 through them for 1 hour.

Hydrogen evolution was monitored by gas chromatography (GC) using a SRI Instruments 8610C Compact GC with a TCD detector and an Alltech Hayesep DB column (30'x 1/8"). Both photochemical reactors were calibrated for H_2 content by the following procedure. Each photoreactor was filled to a set volume of 0.3 M TEA in CH_3CN (315 mL for PR1 and 250 mL for PR2) and deoxygenated with N_2 while stirring. An airtight syringe was used to inject givens amount of hydrogen (0.1 mL to 20 mL) into the photoreactors and then the system was allowed to equilibrate for 30 minutes during which time the solution was continually stirred. A GC sample of 0.5 mL was then taken

using a gas tight syringe and injected into the GC. Nitrogen was used as the carrier gas with a flow rate of 28 mL/min. The column oven and TCD cell were set at temperature of 40ºC and 100ºC respectively. GC. The calibration curves for PR1 and PR2 are shown in Appendix B.

Figure 3.6 Photoreactor used in H_2 production.

3.2.4 Chemical Actinometry

The actinometry procedure was followed as noted in the literature.[80] A 500 mL solution of 0.01 M potassium tris(oxalato)ferrate(III) trihydrate (2.456 g) in 0.05 M H_2SO_4 (1.34 mL) was prepared along with 0.1% solution of phenanthroline (0.1 g phenanthroline to 100 mL of DI water), and a buffer solution consisting of 8.2 g sodium propionate in 99 mL of DI water and 1 mL H_2SO_4. An initial UV spectrum of the ferrioxalate solution was taken, and was then added to the photoreactor according to the set volume for each photoreactor. The ferrioxalate was then irradiated for 10 minutes

with the LED light. A 1 mL aliquot of this irradiated solution was then taken and added to a vial containing 4 mL 0.1% phenanthroline, 0.5 mL buffer, and 4.5 mL DI water. A 1 mL aliquot of ferrioxalate that had not been irradiated was also taken and added to a vial of the same contents for use as a reference. Both solutions were placed in the dark for 1 hour to allow for full color development. A UV spectrum of both solutions was then taken. The photon flux was then calculated for each light source using eq 3.1, where $q_{n,p}$ is the photon flux, Φ is the quantum yield at the excitation wavelength, ε is the molar extinction coefficient for ferrioxalate at 510 nm, and ΔA is the difference in absorbance between the sample and reference. V_1, V_2, and V_3 are dilution factors, while l is the light path length within the photoreactor, and t is the time of irradiation.

$$q_{n,p} = \frac{\Delta A \; V_1 \; V_3}{\Phi \; \varepsilon(510 \text{ nm}) \; V_2 \; l \; t} \qquad \text{Eq. 3.3}$$

The photon flux was found to be 5.3×10^{-7} mol photon/s and 2.5×10^{-7} mol photon/s for photoreactors 1 and 2 respectively.

3.2.5 Monitoring Photo-species in situ

In one photocatalytic reaction, the absorption spectrum of the reaction mixture was monitored by UV absorption over the time course of the experiment. The data were obtained by the following method. At each time point, a 2.5 mL aliquot of the photo-irradiated solution was removed from the photoreactor using a gastight syringe that had been purged with nitrogen. Simultaneously a gas sample was taken for GC analysis. The solution sample was then transferred to a sealed cuvette containing nitrogen, and a UV spectrum was then taken of each respective sample.

3.3 Results and Discussion

3.3.1 Hydrogen Evolution in Acetonitrile

As shown in Figure 3.2, complexes **P** and **Q** are both photochemically reduced to store multiple electrons. The reducing potential of the stored electrons was determined by cyclic voltammetric (CV) under a variety of conditions. In MeCN, these redox processes occur in one-electron steps with **P** reduced at –0.023 V and –0.513 V versus NHE for the P/P^- and P^-/P^{2-} couples. The Q/Q^- and Q^-/Q^{2-} couples are comparable at 0.015 and –0.524 V versus NHE, with the final reductive process being a two-electron couple, Q^{2-}/Q^{4-}, occurring at –1.073 V.[16,20,60] From this data it is apparent that these photocatalysts store a sufficient number of electrons to meet the stoichiometry of the HER and furthermore have a reduction potential that is thermodynamically capable of driving the HER, as shown in equations 3.4 to 3.6.

$$P^{2-} + 2\,H^+ \rightarrow P + H_2 \qquad \Delta G = -52 \text{ kJ/mol} \qquad \text{Eq 3.4}$$

$$Q^{2-} + 2\,H^+ \rightarrow Q + H_2 \qquad \Delta G = -47 \text{ kJ/mol} \qquad \text{Eq 3.5}$$

$$Q^{4-} + 2\,H^+ \rightarrow Q^{2-} + H_2 \qquad \Delta G = -207 \text{ kJ/mol} \qquad \text{Eq 3.6}$$

These free energies were estimated by averaging the 2 one-electron couples in P/P^- and P^-/P^{2-} to $E_{avg} = 0.26$ V for the P^{2-}/P couple and similarly for Q/Q^{2-} at $E_{avg} = -0.25$ V. Actual free energies will be less negative as the presence of protons (in the form of triethylammonium) will undoubtedly shift the potentials to less favorable values.

Under the photochemical conditions that lead to their reduction, both **P** and **Q** show minimal H_2 producing activity thus we examined the addition of co-catalysts to help liberate the stored H_2. Late transition metals, such as Ni, Pd and Pt are often employed as hydrogen evolving co-catalysts, and we chose the simple $M(bpy)Cl_2$

complex shown in Figure 3.7 for our initial screen. Additional parameters such as concentration of the sacrificial reductant [TEA], and the [H^+] were also examined for their effect on the hydrogen generating capability of this system. In the absence of external proton sources, the concentration of H^+ in CH_3CN would be limited to that generated by the decomposition of TEA^+.[51]

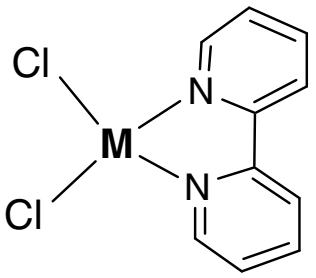

co-catalyst 1: $Ni(bpy)Cl_2$
co-catalyst 2: $Pd(bpy)Cl_2$
co-catalyst 3: $Pt(bpy)Cl_2$

Figure 3.7 General co-catalyst used in H_2 evolution.

Table 3.1 Photocatalytic Evolution of H_2 From **Q** in CH_3CN at 21°C.

Run	$C_{\mathbf{Q}}$ (μM)	co-cat	catalyst mol ratio (**Q**:co-cat)	C_{TEA} (mol L^{-1})	$C_{TEAHPF6}$ (mol L^{-1})	t_{irrad} (h)	TON[a]
1	47	2	10:1	0.30	0	48	0.80
2[b]	47	2	10:1	0.30	0	dark	0
3	47	2	10:1	0.20	0.1	48	0.01
4	47	2	10:1	0.25	0.05	48	2.23[c]
5	47	2	10:1	0.30	0.01	48	1.84
6	47	2	10:1	1.0	0.01	48	0.31
7	47	2	1:10	0.30	0.01	48	0[d]
8	47	2	1:1	0.30	0.01	48	0[d]
9	47	2	20:1	0.30	0.01	48	0.51
10	75	2	10:1	0.30	0.01	48	0.37
11	75	3	10:1	0.30	0.01	48	1.24
12	47	1	10:1	0.30	0.01	48	0.11
13	47	3	10:1	0.30	0.01	48	0[e]
14	47	3	2:1	0.30	0.01	48	26.9
15	47	3	1:1	0.30	0.01	48	33.0

[a] Turnover number (TON) = mol H_2 mol^{-1} catalyst. [b] Sample without irradiation for 25 h. [c] H_2 evolution stopped at 48 hrs due to Pd precipitation. [d] Pd precipitated with increasing concentration upon photo irradiation. [e] Pt was doubled after run, and H_2 evolved.

Hydrogen was formed under numerous conditions that were varied to determine optimal performance with the principle figure of merit being turnover number (TON), which indicates the moles of H_2 formed per mol **Q**. The data from these studies are summarized in Table 3.1. Run 1 shows that H_2 is formed in a simple system of **Q**, co-catalyst 2, and TEA however the TON is less than 1. To verify that the reaction is light-driven, run 2 was performed in the dark and no H_2 was observed even after 24 h. If this solution is then irradiated, H_2 is formed.

One reason why only a small amount of H_2 was produced under the conditions of run 1, was that the $[H^+]$ was limited to that evolved via the decomposition of TEA^+. We

reasoned that an external proton source would improve the H_2 yield. From the data obtained in runs 3-5, we observe that addition of $TEAH^+$ does indeed improve the H_2 yield but only under certain conditions as indicated in Figure 3.8. Initially higher [$TEAH^+$] gave an increased TON but at the highest concentration (0.1M) the proton source shuts down the photochemical activity by catalyst precipitation. In these reactions, the total TEA concentration was held constant at 0.3 M (taking into consideration the TEA produced from the proton source) as a means of comparison.

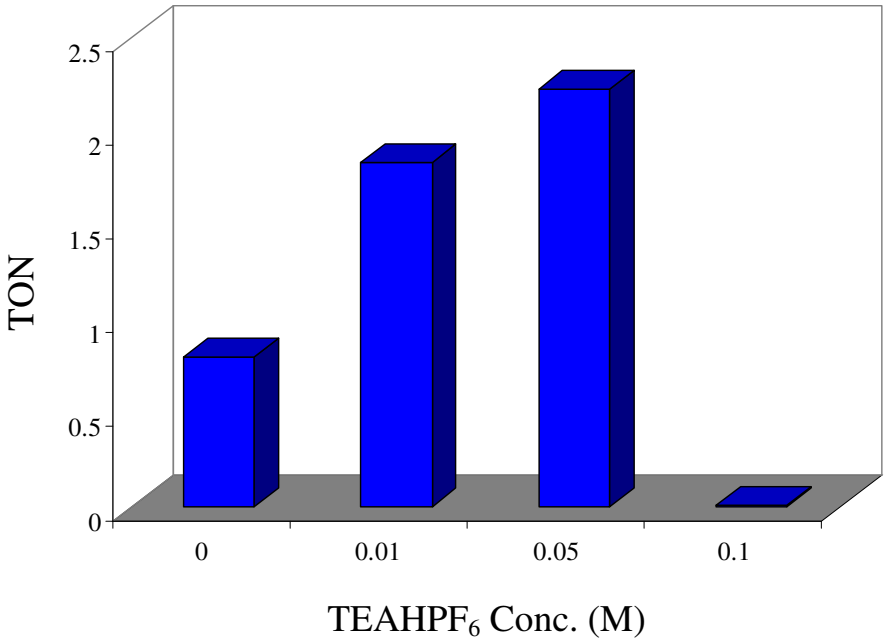

Figure 3.8 H_2 evolution vs. $TEAHPF_6$ concentration.

Increasing the amount of TEA or photocatalyst (runs 6 and 10) within this system resulted in a decrease in H_2 production. The amount of co-catalyst was varied in order to determine the optimum molar ratio of **Q**: co-catalyst (runs 1, 5, 7-9). It was found that

increasing the Pd catalyst past a ratio of 10:1 resulted in the precipitation of the Pd (Figure 3.9).

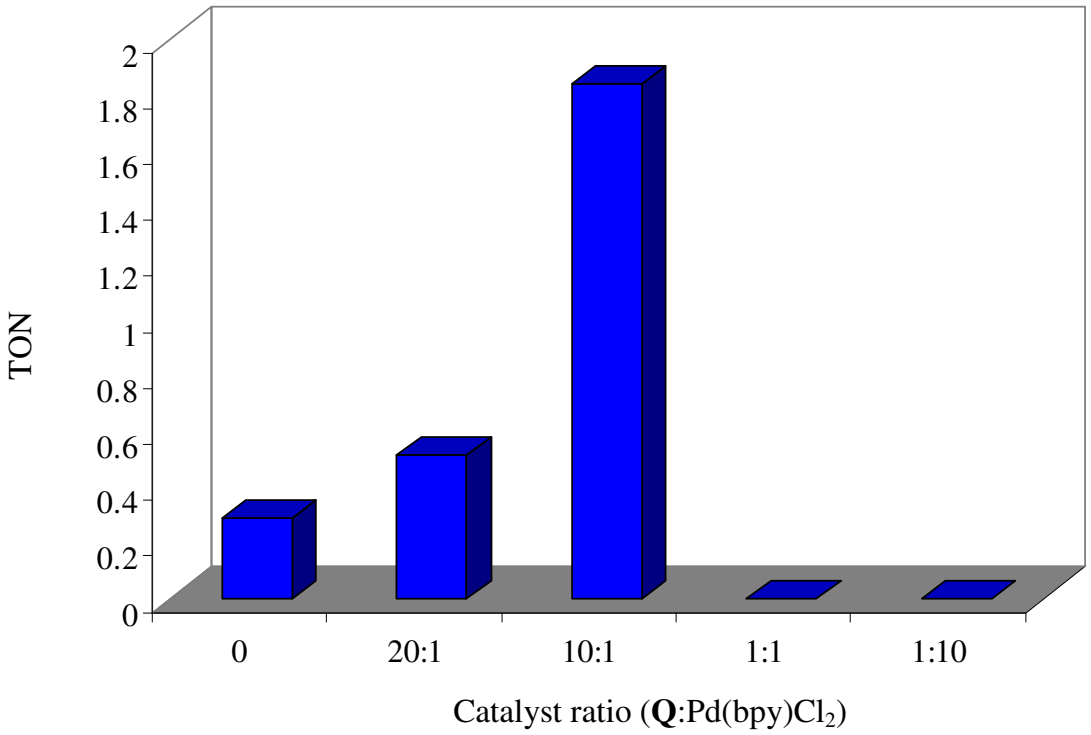

Figure 3.9 H_2 evolution vs. Pd co-catalyst molar ratio.

$Pt(bpy)Cl_2$ and $Ni(bpy)Cl_2$ were also examined as co-catalysts within this system under the optimized conditions of 0.3 M TEA, 0.01 M $TEAHPF_6$, and a catalyst ratio of 10:1 (**Q**: co-cat) as found in runs 12 and 13. The Ni co-catalyst proved to be rather inefficient, while the Pt was not able to produce any H_2 (Figure 3.10). It was found that doubling the amount of Pt co-catalyst in run 13 resulted in H_2 evolution. In runs 13-15, the molar ratio of **Q**: Pt co-catalyst was varied to determine the optimum condition (Figure 3.11).

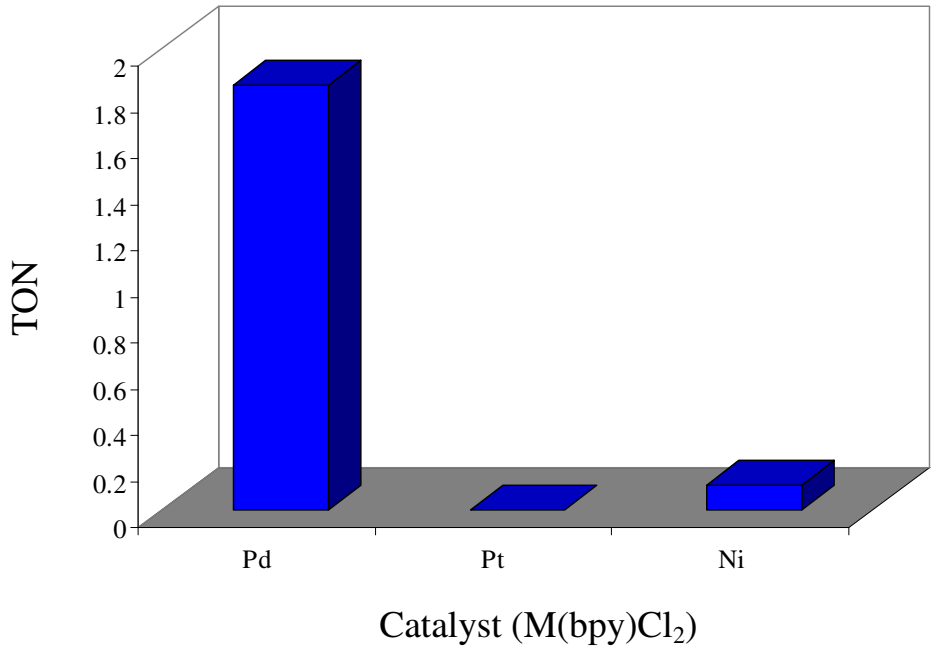

Figure 3.10 H_2 evolution vs. catalyst at 10:1 **Q:**co-catalyst ratio.

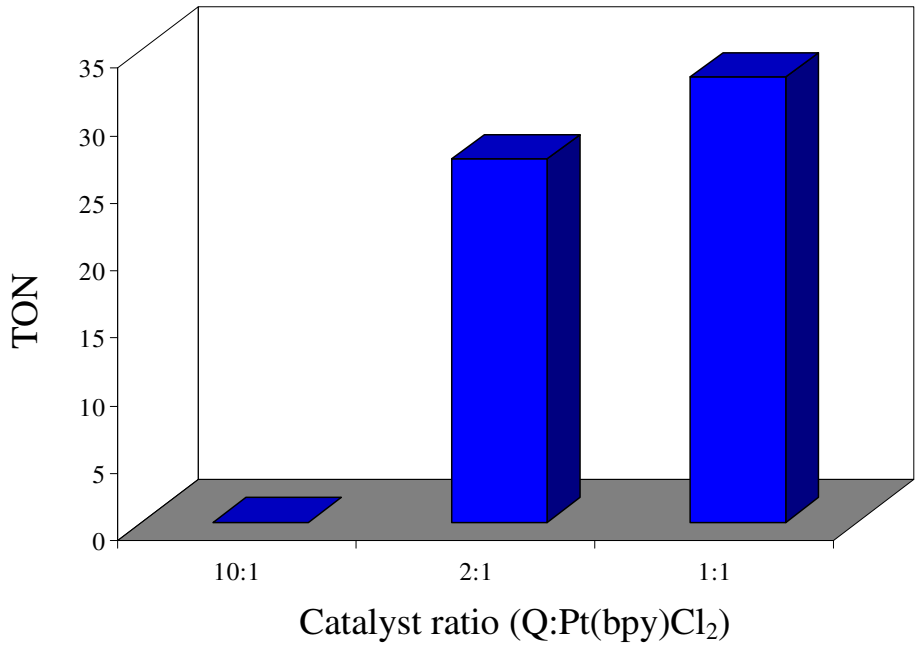

Figure 3.11 H_2 evolution vs. Pt co-catalyst molar ratio.

Table 3.2 H_2 Evolution Under Optimized Conditions.*

Photo-cat.	co-cat	t_{irrad} (hrs)	TON
$[Ru(bpy)_3]^{2+}$	$Pt:MV^{2+}$	22	108
$[Ru(bpy)_3]^{2+}$	Pt	22.5	74.2
Q	Pt	220	66.4
P	Pt	48	18.5
Q	-	48	0.3
P	-	48	0.3
-	Pt	48	3.0

*All photocatalysts and co-catalysts are 47 μM
with 0.3 M TEA and 0.01 M $TEAHPF_6$ in CH_3CN.

It is clear that either **P** or **Q** is an essential component for efficient H_2 evolution within this system (Table 3.2). Small amounts of H_2 were produced when **P** and **Q** were used without a co-catalyst. The co-catalyst also evolved small amounts of H_2, but when **P** or **Q** and the co-catalyst were used together, a significant increase in H_2 production occurred. Complex **Q** proved to be a slightly better photocatalyst than **P**, thus it was utilized during the optimization of the reaction conditions found in Table 3.1. Under these optimized conditions, a turnover number of 66.4 mol H_2 per mol catalyst was found for the complex **Q** after irradiation for 220 h.

The standard photocatalytic system of $[Ru(bpy)_3]^{2+}$, MV^{2+}, a sacrificial reducing agent, and a Pt catalyst has been studied extensively[81] and serves as a good point of reference for **P** and **Q**. This standard system was run under the same conditions and yielded a TON of 108, but it stopped producing H_2 after 22 h. The electron relay, MV^{2+}, was removed from this system and ran under the same conditions to determine the impact this electron relay has on the efficiency of this system. When $[Ru(bpy)_3]^{2+}$ and $Pt(bpy)Cl_2$ are run together under the conditions noted above, it resulted in a TON of 74.2 and had a catalytic lifetime of 22.5 h. The presence of this electron relay increases the

efficiency of this system by approximately ½, but the system still functions rather efficiently in its absence. Presumably, the presence of the bipyridine ligand on the Pt co-catalyst is able to mediate the electron transfer from the excited $[Ru(bpy)_3]^{2+*}$ state to the Pt co-catalyst. This result has also been reported for a system containing $[Ru(bpy)_3]^{2+}$, ascorbic acid, and $[Co(bpy)]^{2+}$ or $[Co(bpy)_2]^{2+}$.[82]

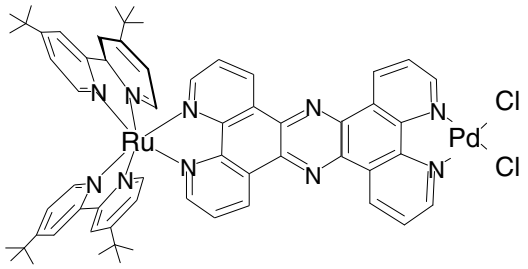

Figure 3.12 Heterodinuclear Ru-Pd complex.

The heterodinuclear Ru-Pd complex (Figure 3.12) reported by Rau et al. was found to evolve H_2 under conditions similar to that used for complex **Q**. H_2 was produced in 2 M TEA in CH_3CN with a TON of 56.4. This complex stopped producing H_2 after 30 h, much like what was found for $[Ru(bpy)_3]^{2+}$. The amount of H_2 evolved is comparable for all three photocatalysts, but the major difference is the amount of time **Q** can be irradiated before it stops producing H_2.

The quantum yield (**Φ**) for photocatalytic processes is generally reported in terms of mol of product per mol of photons absorbed. In the case of photocatalytic H_2 production, it is commonplace to report the **Φ** as mol of e^- per mol of photons absorbed. Since H_2 evolution is a two-electron process, the amount of H_2 produced is doubled to get the mol of e^-. The final quantum yields for the reactions with **Q** are lower due to the

ability of these photocatalysts to produce H_2 for long periods of time. As the irradiation time increases, the number of photons absorbed increases, thus making the **Φ** decrease over time (Figure 3.13).

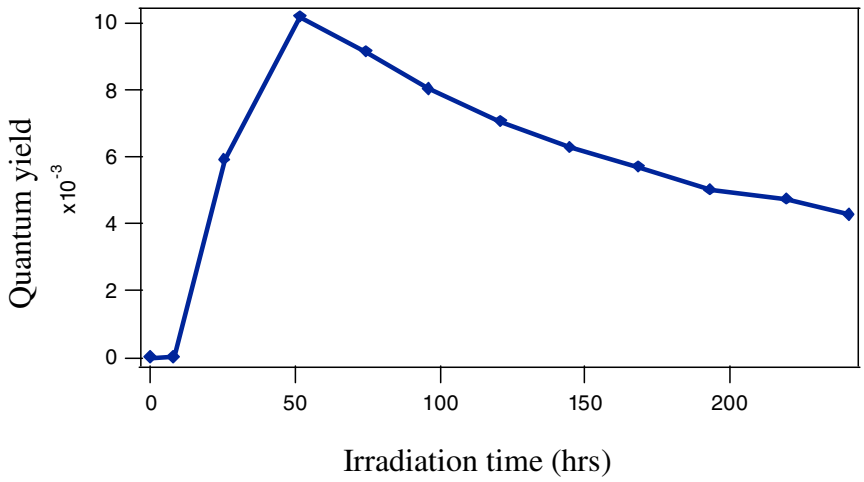

Figure 3.13 Quantum yield for H_2 production from **Q**.

The **Φ** for the reaction with $[Ru(bpy)_3]^{2+}$ is approximately 10 times greater than that for complex **Q** due to the short amount of time that it was able to evolve its H_2. The largest increase in H_2 production for **Q** takes place between 24 and 48 h, which corresponds to the highest **Φ** value.

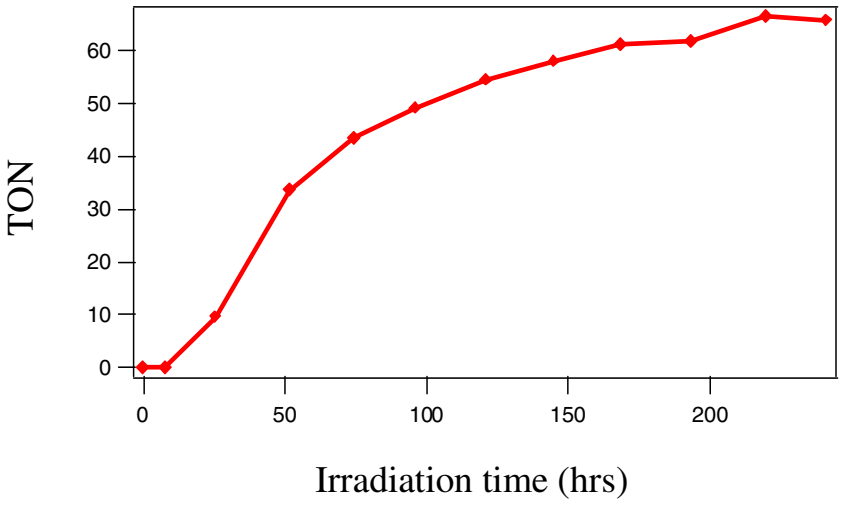

Figure 3.14 H_2 evolution vs. irradiation time of **Q.**

Within this photocatalytic system, H_2 production is not detected until 6-8 h after photo irradiation has begun (Figure 3.14). This lag period is thought to be due to the nature of the Pt co-catalyst, and its propensity to form colloidal particles. Due to the low to moderate solubility of $Pt(bpy)Cl_2$ in CH_3CN at 21°C, these Pt colloidal particles require a few hours to form before H_2 can begin. This same lag period occurred when the Pt co-catalyst was run by itself. However, in the case of $[Ru(bpy)_3]^{2+}$, there was no lag period. This phenomenon is likely due to the differences in reduction potentials. The first two reductive processes of **P** and **Q** both come at lower potentials than that of $[Ru(bpy)_3]^{2+}$. The $Pt(bpy)Cl_2$ is sufficient to liberate H_2 coupled with the reductive power of $[Ru(bpy)_3]^{2+}$ but unable to function with lower reduction potentials. Over time upon photo irradiation, this leads to the formation of Pt colloids that can efficiently function with **Q** or **P** to evolve H_2. A similar lag period and subsequent Pt colloid formation during catalytic H_2 evolution has been previously investigated and reported in the literature.[83]

3.3.2 Stability of the Reduced Photocatalyst

The standard photocatalyst $[Ru(bpy)_3]^{2+}$ was run under the same conditions as **P** and **Q** and resulted in a total amount of H_2 that was approximately 8 turnovers more than that for **Q**. The most significant part of the comparison between $[Ru(bpy)_3]^{2+}$ and **Q** is the vast difference in the stability of these photocatalyst. Upon photoirradiation under the given conditions in table 3.2, $[Ru(bpy)_3]^{2+}$ stopped producing H_2 after 22.5 hrs. The photo decomposition of $[Ru(bpy)_3]^{2+}$ occurs through the mechanism of ligand dissociation in which the ruthenium based d-d states that occur 43 kJ/mol higher in energy than the ^{3}MLCT state is populated leading to photolabilization of the ligands.[74,75] Many photocatalyst decompose within 20 to 30 h of irradiation, but in the case of complex **Q**, it has been proven to be much more stable (Figure 3.15). Under the given conditions in table 3.2, **Q** was irradiated and produced H_2 for 9 days. When H_2 evolution ceased, the reaction mixture was the characteristic green color of reduced **Q**, and within minutes of exposing this solution to air it was oxidized back to its original red color. This suggests that **Q** is still photoactive, and that the co-catalyst is the limiting factor in this system.

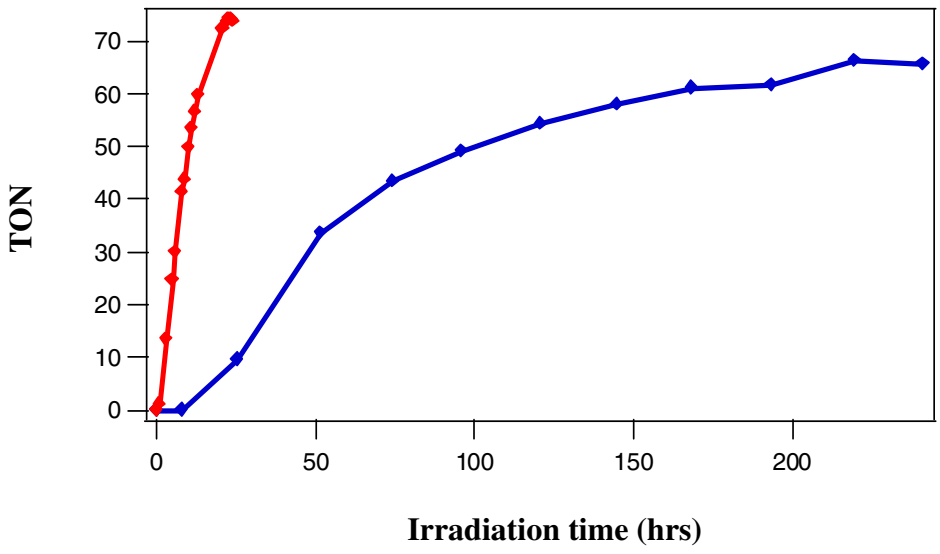

Figure 3.15 Photocatalytic lifetime. (— $[Ru(bpy)_3]^{2+}$, — **Q**)

3.3.3 Monitoring Photo-irradiated Solution by UV

The evolution of the absorption spectrum of **Q** was monitored over the time course of the hydrogen-evolving experiment by periodically withdrawing an aliquot of the reaction solution and examining the electronic absorption spectrum. The same conditions were used as noted in table 3.2. The total amount of H_2 produced and the photocatalytic lifetime of the system were both less than the values observed when this system was allowed to run undisturbed. This is due to the removal of UV samples, which decreased the total amount of catalyst present and could also have interfered with colloid formation in the beginning stages of this experiment. Despite lower results, the objective of this experiment was still achieved. The UV spectra (Figure 3.16) and subsequent GC data (Figure 3.17) provide a glimpse of the photo-activity of this system during H_2 evolution.

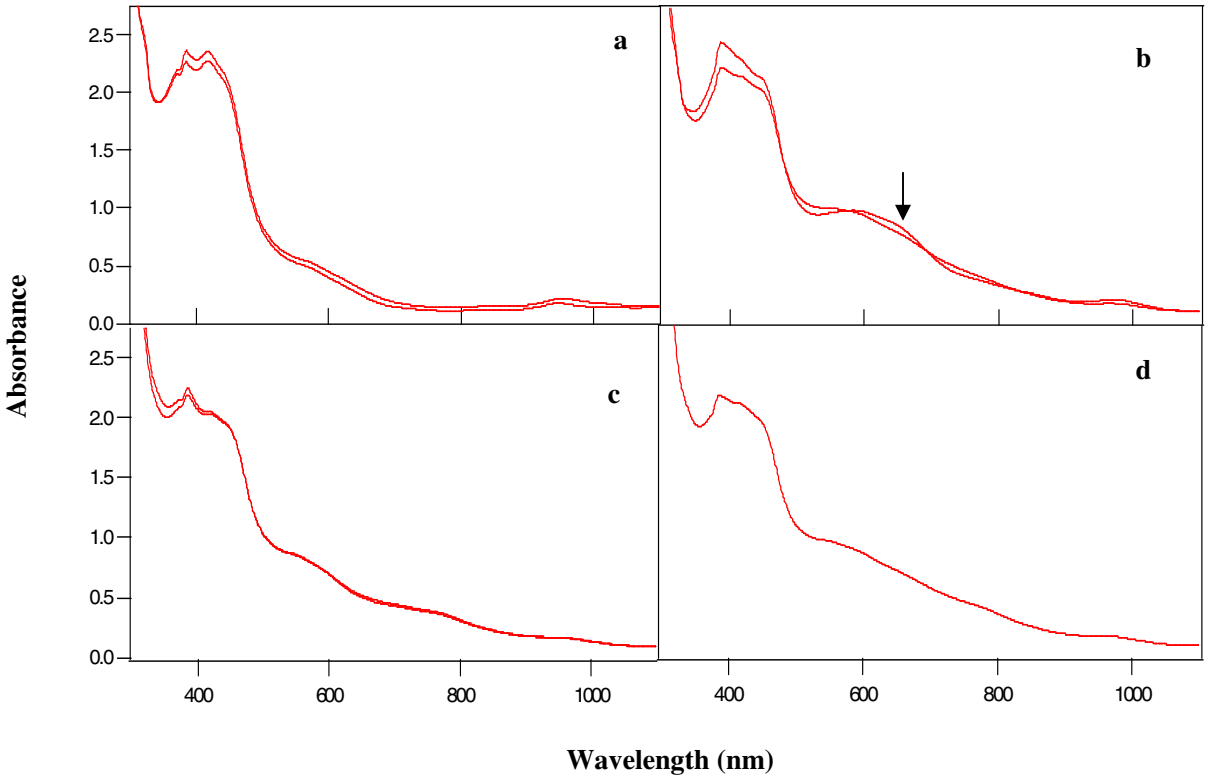

Figure 3.16 Evolution of the visible spectrum during H_2 evolution.
a) 0 h, b) 24 to 48 h, c) 72 to 120 h, d) final complex.

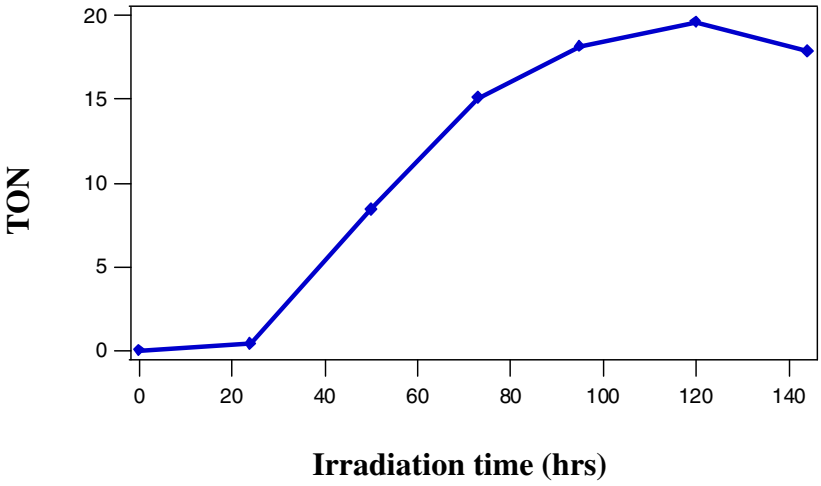

Figure 3.17 H_2 evolution vs. time during UV experiment.

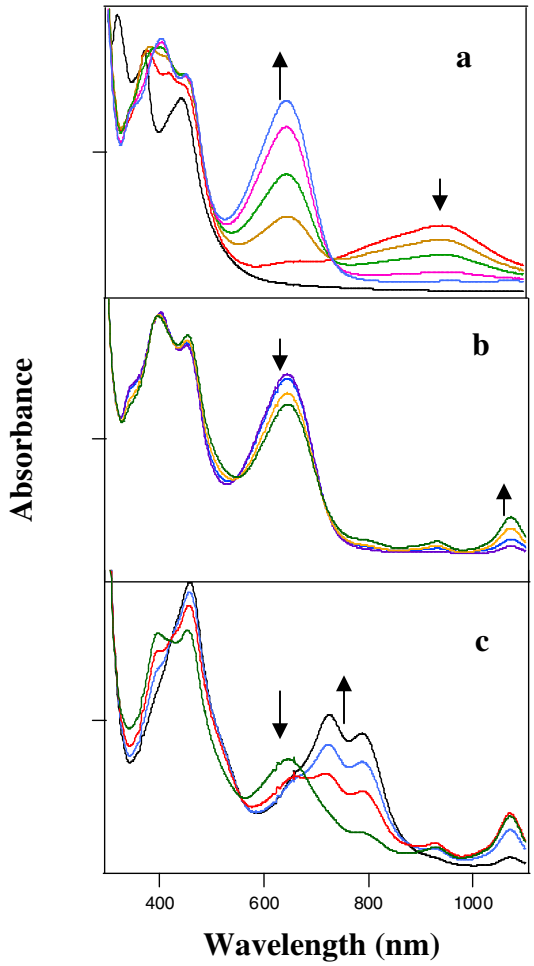

Figure 3.18 Evolution of the visible spectrum of **Q** observed during photoirradiation. Conditions: CH_3CN, 0.25 M TEA, 23°C. a) The band growing in at 620 nm corresponds to the 2 e^- reduction of **Q** → **H_2Q**.

The initial spectra was taken before irradiation and also after irradiation upon reduction of the solution indicated by a color change from red to green. These spectra are shown in Figure 3.16a. In order to minimize the amount of solution removed from the photoreactor for UV data, only one sample was taken each day. During H_2 evolution, there is a noticeable shift in the UV spectra at 600 nm. This peak corresponds to the 2 e^- reduction of **Q** that is observed during photo irradiation in the presence of a sacrificial reducing agent (Figure 3.18). This peak is observable in the initial spectra due to a partial

reduction of the solution from ambient light during sample preparation. Even though the sample is reduced, there is no H_2 produced at this initial stage. The absorbance at 600 nm is the most intense at 24 and 48 h, which corresponds to the time period that the solution was producing the most H_2. From 48 to 120 h, H_2 production slows down and levels off, while the band at 600 nm sinks to a point in between the initial and 24 h spectra and stays steady during this period. Once H_2 production ceased at 120 h, the intensity of the band at 600 nm increased to a point between the 24 hr and 72 h spectra. Even after continued photo irradiation, this inactive complex maintained the same UV spectra shown in Figure 3.16d. The relative intensity of this spectral band at 600 nm corresponds well to the rate of H_2 production as shown in Figure 3.17.

In order to determine if **Q** was still in tact, the contents of the reaction mixture were recovered after it had stopped evolving H_2. The majority of the solvent was removed by rotary evaporation and the catalyst precipitated by the addition of water. The solid that was collected was examined by ^{1}H NMR and ESI-MS. The NMR results appeared to be paramagnetic, and while peaks were present that are characteristic of **Q**, the results were not conclusive. Due to the Pt complexes in solution, there were a number of peaks shown on the ESI-MS, but **Q** was present (Appendix C). With many other peaks present, it is possible that some of the complex **Q** could have degraded. The final fate of **Q** within this system is not known, but some amount of **Q** was still in the final solution, which was still photoactive.

3.3.4 Hydrogen Evolution in Aqueous Media

In order for a photocatalyst to be a viable choice in solar H_2 production from water, it must be able to function in an aqueous solution. Complexes **P** and **Q** have both been shown to photoreduce in water in the presence of a sacrificial reducing agent. Using K_2PtCl_4 as the co-catalyst in a 1:1 molar ratio, the photocatalytic ability both **P** and **Q** in water were tested. A 47 μM solution of **P** and **Q** in water were both prepared. The solution was 1 M TEA with a pH of 11.5. Upon photo irradiation, both solutions began to slowly evolve H_2. The Pt co-catalyst was also run under the same conditions by itself to determine the amount of H_2 it produces by itself (Table 3.3).

Table 3.3 H_2 Evolution in Aqueous Media.*

Photo-cat.	**co-cat.**	**TON**
Q	Pt	0.92
P	Pt	0.80
-	Pt	0.47

* all solutions were irradiated for 48 h

The amount of H_2 produced is not much but given the high pH and unfavorable conditions, it is still a significant result. The $[Ru(bpy)_3]^{2+}$, $Pt(II)Cl_2$ complex (Figure 3.19) reported by Sakai et al.[79] has been reported to evolve H_2 with a TON of 4.8 from an aqueous EDTA, acetate buffer solution at pH 5. These reaction conditions are more favorable for H_2 production than those used for the initial screening of **P** and **Q**, and yet only a small amount of H_2 is produced from this complex.

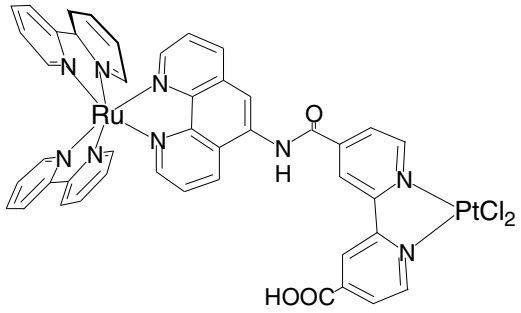

Figure 3.19 $[Ru(bpy)_3]^{2+}$, $Pt(II)Cl_2$ complex.

The reaction conditions for **P** and **Q** need to be optimized from this point. TEA concentration, pH, various co-catalyst, and catalyst concentration are all parameters that need to be adjusted to optimize the photocatalytic ability of **P** and **Q**.

3.4 Conclusion

Complexes **P** and **Q** proved to be suitable photocatalysts in terms of overall H_2 production, but in terms of longevity, they proved to be much more stable than most photocatalyst. When compared to similar photocatalyst, **P** and **Q** are able to produce equivalent overall amounts of H_2, but in each case are able to produce H_2 for much longer periods of time. The heterodinuclear Ru-Pd complex reported by Rau et al. was able to produce H_2 with a TON = 56.4 in CH_3CN, while **Q** gave a TON = 66.4. Rau's complex was said to stop producing H_2 after 30 hrs, while **Q** lasted 9 days. The complex reported by Sakai et al. was able to produce H_2 in water with a low TON only slightly larger than that of **P** and **Q**.

Both systems in CH_3CN are found to produce approximately the same amount of H_2, but **P** and **Q** require a longer period of time to do it. In this sense, the total amount of H_2 produced from **P** and **Q** is not overwhelming. It simply shows the functionality and ability of these compounds to act as photocatalyst. The stability of these complexes, on

the other hand, is very promising in the sense that they show a longevity and resistance to photodecomposition unlike any other photocatalyst. This serves as a basis from which this system can be improved upon, and this family of complexes can be further investigated in order to enhance H_2 production while utilizing the stability of these compounds.

APPENDIX A

UV-VIS SPECTRA OF **tP** AND **tQ**

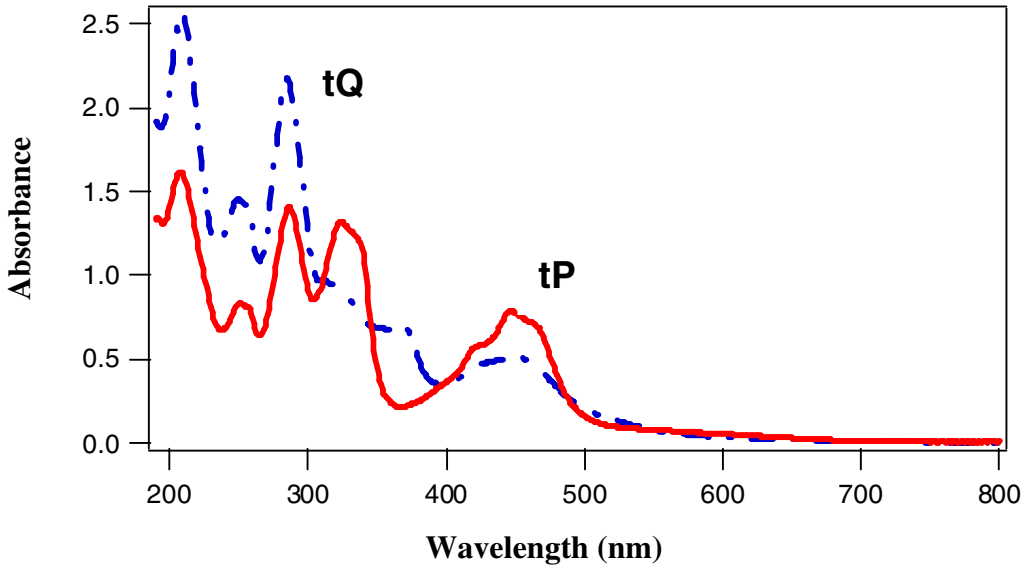

UV-VIS spectra of **tP** and **tQ**. 15.6 μM in CH_3CN.

APPENDIX B

HYDROGEN CALIBRATION CURVES FOR PHOTOREACTORS 1 AND 2.

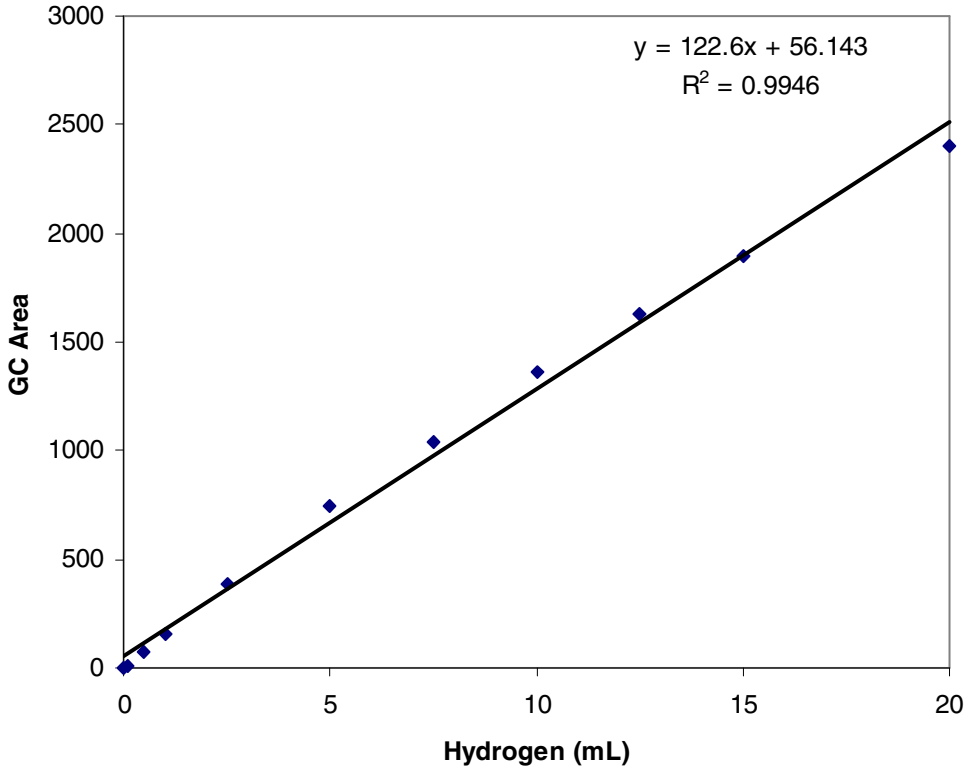

Hydrogen Calibration Curve for PR1.

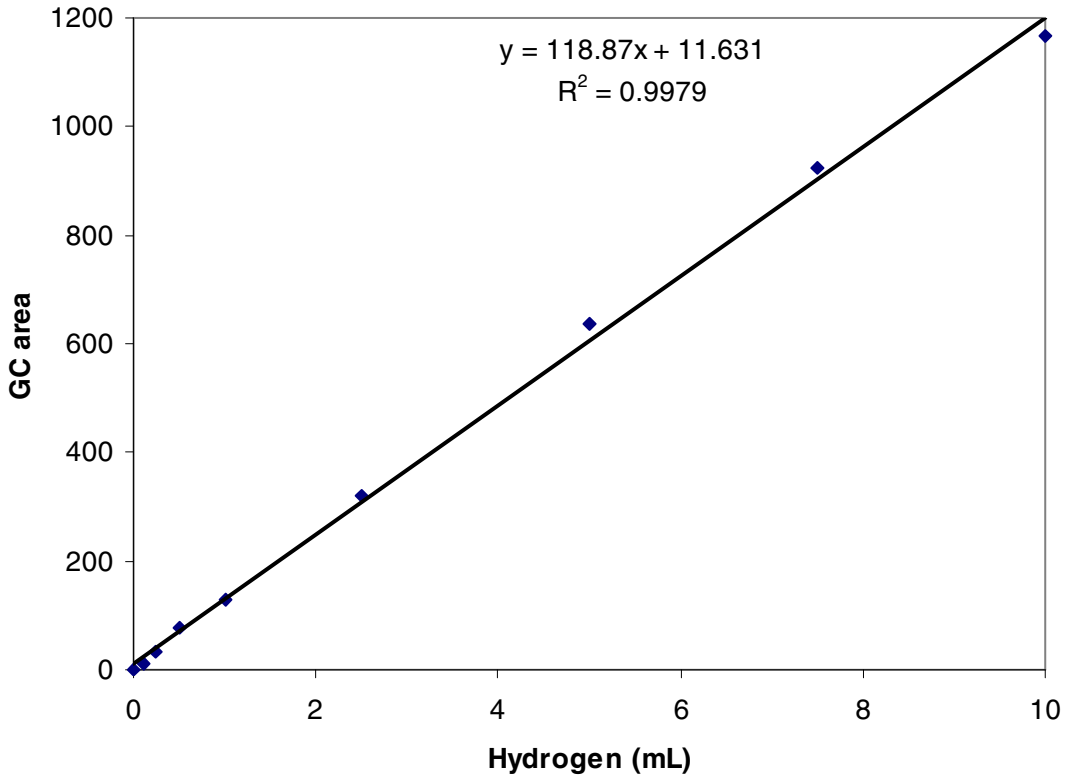

Hydrogen Calibration Curve for PR2.

APPENDIX C

ESI-MS OF PHOTOIRRADIATED **Q** SOLUTION

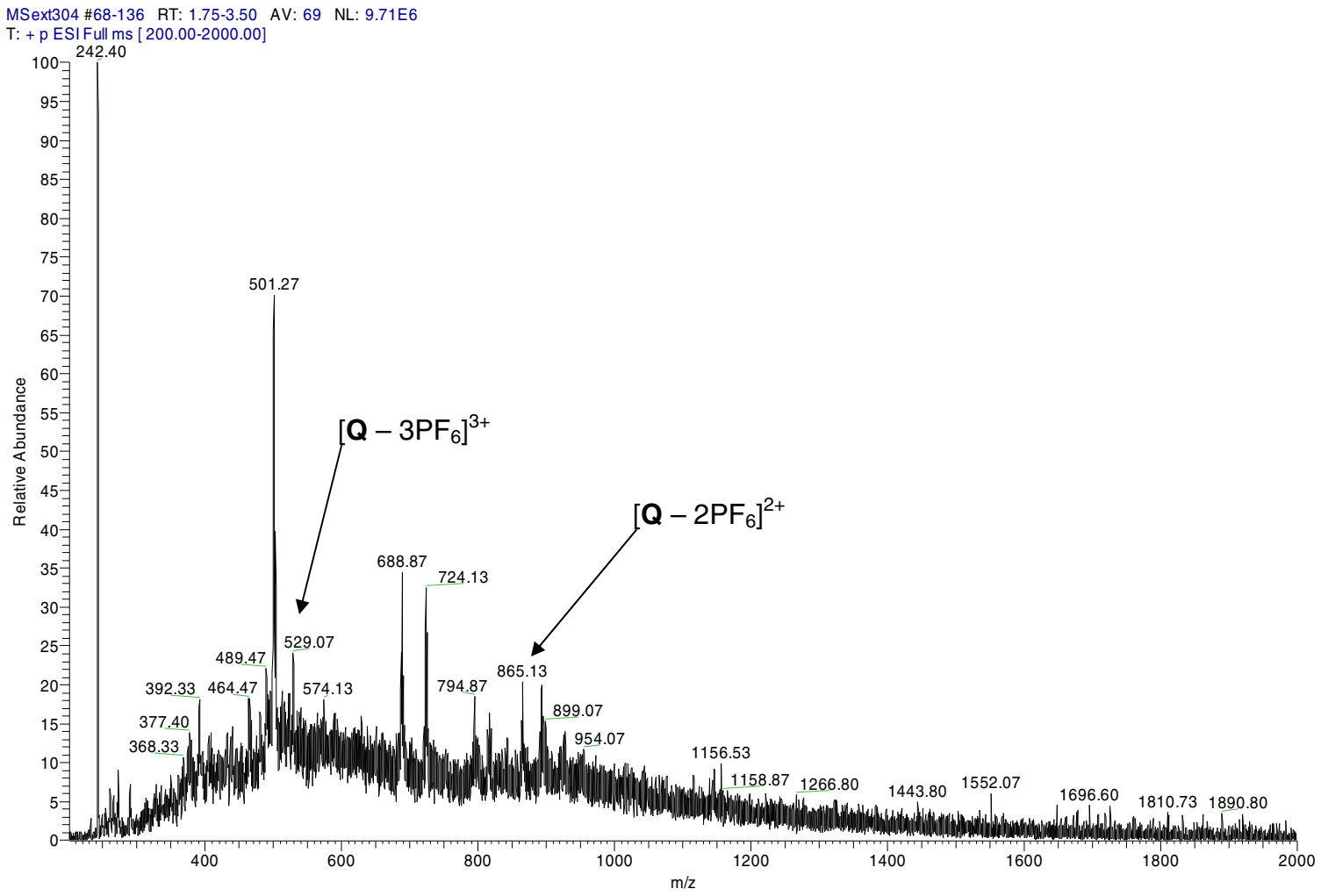

ESI-MS Photoirradiated **Q** Solution

REFERENCES

(1) In *Basic Research Needs for Solar Energy Utilization*; US DOE - Basic Energy Sciences: http://www.sc.doe.gov/bes/reports/, 2005.

(2) In *Basic Research Needs for the Hydrogen Economy*; US DOE - Basic Energy Sciences: http://www.sc.doe.gov/bes/reports/, 2003.

(3) Schlapbach, L.; Zuttel, A. *Nature* **2001**, *414*, 353-358.

(4) Turner, J. A. *Science* **1999**, *285*, 687.

(5) Jacoby, M. In *Chemical and Engineering News* May 30, 2003; Vol. 33, p 35-37.

(6) Lewis, N. S. *Nature* **2001**, *414*, 589-590.

(7) Dresselhaus, M. S.; Thomas, I. L. *Nature* **2001**, *414*, 332-337.

(8) Danks, S. M. *Photosynthetic Systems : Structure, Function, and Assembly*; Wiley: New York, 1983.

(9) Conolly, J. S. *Photochemistry Conversion and Storage of Solar Energy* **1981**, *Acedemic Press*.

(10) Toshifumi, K.; Ikeda, A.; Shinkai, S. *Tetrahedron* **2005**, *61*, 4881-4899.

(11) Chakraborty, S.; Wadas, J. T.; Hester, H.; Schmehl, R.; Eisenberg, R. *Inorg. Chem.* **2005**, *44*, 6865-6878.

(12) Alstrum-Acevedo, J. H.; Brennaman, M. K.; Meyer, T. J. *Inorg. Chem.* **2005**, *44*, 6802-6827.

(13) Deisenhofer, J.; Epp, O.; Miki, K.; Huber, R.; Michel, H. *J. Mol. Bio.* **1984**, *180*, 385-98.

(14) Villegas, J. M.; Stoyanov, S. R.; Rillema, D. P. *Inorg. Chem.* **2002**, *41*, 6688.

(15) Beyeler, A.; Besler, P. *Coord. Chem. Rev.* **2002**, *230*, 29.

(16) Kim, M.-J.; Konduri, R.; Ye, H.; MacDonnell, F. M.; Puntoriero, F.; Serroni, S.; Campagna, S.; Holder, T.; Kinsel, G.; Rajeshwar, R. *Inorg. Chem.* **2002**, *41*, 2471-2476.

(17) Sendt, K.; Johnson, L. A.; Hough, W. A.; Crossley, M. J.; Hush, N. S. *J. Am. Chem. Soc.* **2002**, *124*, 9299.

(18) Crossley, M. J.; Johnson, L. A. *Chem. Commun.* **2002**, 1122.

(19) Galland, B.; Limosin, D.; Deronzier, A.; Helene, L. P. *Inorg. Chem.* **2002**, *5*, 5.

(20) Konduri, R.; Ye, H.; MacDonnell, F. M.; Serroni, S.; Campagna, S.; Rajeshwar, K. *Angew. Chem. Int. Ed.* **2002**, *41*, 3185-3187.

(21) Gratzel, M. *Nature* **2001**, *414*, 303.

(22) Brian, C. H.; Angelika, H. *Nature* **2001**, *414*, 345.

(23) Fujishima, A.; Honda, K. *Nature* **1972**, *37*, 238.

(24) Kato, H.; Kudo, A. *J. Phys. Che. B* **2001**, *105*, 4285-4292.

(25) Kato, H.; Asakura, K.; Kudo, A. *J. Am. Chem. Soc.,* **2003**, *125*, 3082-3089.

(26) Serway, R.; Beichner, R. *Physics for Scientists and Engineers with Modern Physics*; 5th ed.; Saunders College Publishing: Orlando, 2000.

(27) Amouyal, E. *Solar Energy Materials and Solar Cells* **1995**, *38*, 249-76.

(28) Hoertz, P. G.; Mallouk, T. E. *Inorg. Chem.* **2005**, *44*, 6828 -6840.

(29) Manchanda, R.; Brudvig, G. W.; Crabtree, R. H. *Coord. Chem. Rev.* **1995**, *144*, 1-38.

(30) Balzani, V.; Juris, A.; Venturi, M.; Campagna, S.; Serroni, S. *Chem. Rev.* **1996**, *96*, 759-833.

(31) Willner, I.; Kaganer, E.; Joselevich, E.; Dorr, H.; David, E.; Gunter, M. J.; Johnston, M. R. *Coord. Chem. Rev.* **1998**, *171*, 261-285.

(32) Hissler, M.; McGarrah, J. E.; Connick, W. B.; Geiger, D. K.; Cummings, S. D.; Eisenberg, R. *Coor. Chem. Rev.* **2000**, *208*, 115-137.

(33) Dempsey, J. L.; Esswein, A. J.; Manke, D. R.; Rosenthal, J.; Soper, J. D.; Nocera, D. G. *Inorg. Chem., 44 (20), ,* **2005**, *44*, 6879 -6892.

(34) Wasielewski, M. R. *Chem. Rev.* **1992**, *92*, 435-461.

(35) Cole-Hamilton, D. J.; Bruce, D. W. In *Comp. Coord. Chem. V. 6*; Wilkinson, G., Gillard, R. D., McCleverty, J. A., Eds.; Pergamon Books Ltd: Maxwell House, NY, 1987; Vol. 6.

(36) Kodis, G.; Liddell, P. A.; de la Garza, L.; Clausen, P. C.; Lindsey, J. S.; Moore, A. L.; Moore, T. A.; Gust, D. *J. Phys. Chem. A.* **2002**, *106*, 2036 - 2048.

(37) Kutal, C. J. *Chem. Educ.,* **1983**, *60*, 882.

(38) Kaneko, M.; Yamada, A. *Photochem. Photobiol.,* **1981**, *33*, 793.

(39) Rougee, M.; Ebbesen, T.; Bensasson, R. V. *J. Phys. Chem.,* **1982**, *86*, 4414.

(40) Harriman, A.; Porter, G.; Richoux, M. C. *J. Chem. Soc., Faraday Trans. II* **1981**, *77*, 833.

(41) Swarnkar, M.; Gupta, M.; Nema, S. K. *International Journal of Hydrogen Energy* **1997**, *22*, 989-993.

(42) Juris, A.; Balzani, V.; Barigelletti, F.; Campagna, S.; Belser, P.; Von Zelewsky, A. *Coord. Chem. Rev.* **1988**, 85-277.

(43) Kober, E. M.; Meyer, T. J. *Inorg. Chem.* **1982**, *21*, 3967-3977.

(44) Kober, E. M.; Meyer, T. J. *Inorg. Chem.* **1983**, *221*, 1614-1616.

(45) Kober, E. M.; Caspar, J. V.; Sullivan, B. P.; Meyer, T. J. *Inorg. Chem.* **1988**, *27*, 4587-4598.

(46) Crosby, G. A.; Striplin, D. R. *Chem. Phys. Lett.,* **1994**, *221*, 426-430.

(47) Meyer, T. J. *Pure Appl. Chem.* **1986**, *58*, 1193.

(48) Kelch, S.; Rehahn, M. *Macromolecules* **1997**, *30*, 6185-6193.

(49) Strouse, G. F.; Anderson, P. A.; Schoonover, J. R.; Meyer, T. J.; Keene, F. R. *Inorg. Chem.* **1992**, *31*, 30004-3006.

(50) Sullivan, B. P.; Calvert, J. M.; Meyer, T. J. *Inorg. Chem.* **1980**, *19*, 1404-1407.

(51) DeLaive, P. J.; Foreman, T. K.; Giannotti, C.; Whitten, D. G. *J. Am. Chem. Soc.* **1980**, *102*, 5627-5631.

(52) Demas, J. N.; Addington, J. W. *J. Am. Chem. Soc.* **1976**, *98*, 5800-5806.

(53) Bolleta, F.; Juris, A.; Maestri, M.; Sandrini, D. *Inorg. Chim. Acta.* **1980**, *44*, L175-L176.

(54) Sutin, N. *Photochem.* **1979**, *10*, 19.

(55) Watts, R. J. *Comm. Inorg. Chem.* **1991**, *11*, 303-337.

(56) Meyer, T. J. *J. Electrochem. Soc.* **1984**, 221C-228C.

(57) Molnar, S. M.; Nallas, G.; Bridgewater, J. S.; Brewer, K. J. *J. Am. Chem. Soc.* **1994**, *116*, 5206-5210.

(58) Brewer, K. J.; Elvington, M. *Supramolecular Complexes as Photocatalysts for the Production of Hydrogen from Water.* **2006**, *US 7,122,171 B2*.

(59) de Tacconi, N. R.; Lezna, R. O.; Konduri, R.; Ongeri, F.; Rajeshwar, K.; MacDonnell, F. M. *Chem. Eur. J.* **2005**, *Published Online: 11 May 2005*.

(60) Konduri, R.; de Tacconi, N. R.; Rajeshwar, K.; MacDonnell, F. M. *J. Am. Chem. Soc.* **2004**, *126*, 11621-9.

(61) Harrison, A.; Whittaker, A. G. *Comp. Coord. Chem. II,* **2003**, *1*, 741-745.

(62) Lidstrom, P.; Tierney, J.; Wathey, B.; Westman, J. *Tetrahedron* **2001**, *57*, 9225-9283.

(63) Caddick, S. *Tetrahedron.* **1995**, *51*, 10403-10432.

(64) Mingos, D. M.; Baghurst, D. R. *Chem. Soc. Rev.* **1991**, *20*, 1-47.

(65) Baghurst, D. R.; Cooper, S.; Greene, D.; Mingos, D. M.; Reynolds, S. *Polyhedron.* **1990**, *9*, 893-895.

(66) Choudhury, D.; Jones, R. F.; Smith, G.; Cole-Hamilton, D. J. *J. Chem. Soc.,Dalton Trans.* **1982**, 1143.

(67) Rau, S.; Schafer, B.; Grubing, A.; Schebesta, S.; Lamm, K.; Vieth, J.; Gorls, H.; Walther, D.; Rudolph, M.; Grummt, U.; Birkner, E. *Inorg. Chim. Acta.* **2004**, *357*, 4496-4503.

(68) Rau, S.; Ruben, M.; Buttner, T.; Temme, C.; Dautz, S.; Gorls, H.; Rudolph, M.; Walther, D.; Brodkorb, A.; Duati, M.; O'Conner, C.; Vos, J. *J. Chem. Soc.,Dalton Trans.* **2000**, 3649-3657.

(69) Sullivan, B. P.; Salmon, D. J.; Meyer, T. J. *Inorg. Chem.* **1978**, *17*, 3334.

(70) Bennett, M. A.; Wilkinson, G. *Chem. Ind.* **1959**.

(71) Hadda, T. B.; Le Bozec, H. *Polyhedron.* **1988**, *7*, 575.

(72) Pimentel, L.; de Souza, A.; Fernandez, T.; Wardell, J.; Antunes, O. *Tetrahedron Letters.* **2007**, *48*, 831-833.

(73) Balzani, V.; Juris, A. *Coordination Chemistry Reviews* **2001**, *211*, 97-115.

(74) Durham, B.; Caspar, J. V.; Nagle, J. K.; Meyer, T. J. *J. Am. Chem. Soc.* **1982**, *104*, 4803-4810.

(75) Van Houten, J.; Watts, R. J. *Inorg. Chem.* **1978**, *17*, 3381 - 3385.

(76) Chang, C. C.; Pfennig, B.; Bocarsly, A. B. *Coor. Chem. Rev.* **2000**, *208*, 33.

(77) Esswein, A.; Veige, A.; Nocera, D. J. *J. Am. Chem. Soc.* **2005**, *127*, 16641.

(78) Rau, S.; Schafer, B.; Gleich, D.; Anders, E.; Rudolph, M.; Friedrich, M.; Gorls, H.; Hernry, W.; Vos, J. *Angew. Chem. Int. Ed.* **2006**, *45*, 6215-6218.

(79) Sakai, K.; Ozawa, H.; Haga, M. *J. Am. Chem. Soc.* **2006**, *128*, 4926-4927.

(80) Kuhn, H. J.; Braslavsky, S. E.; Schmidt, R. *Pure Appl. Chem.* **2004**, *76*, 2105-2146.

(81) Gratzel, M. *Helv. Chim. Acta.* **1978**, *61*, 2720.

(82) Krishnan, C. V.; Sutin, N. *J. Am. Chem. Soc.* **1981**, *103*, 2141.

(83) Kirch, M.; Lehn, J.-M.; Sauvage, J.-P. *Helv. Chim. Acta.* **1979**, *62*, 1345-1384.

BIOGRAPHICAL INFORMATION

Cale McAlister was born and raised in central Oklahoma. He received his undergraduate degree in chemistry from the University of Oklahoma in 2003. He worked in the research and development department of Sovereign Pharmaceuticals in Fort Worth, TX for a year before pursuing his graduate degree. He received his M.S. degree working with Prof. Fred MacDonnell at the University of Texas at Arlington in the spring of 2007.